Hamburger Beiträge
zur Angewandten Mathematik

Computational Aspects of Pseudospectra in Hydrodynamic Stability Analysis

D. Gerecht, R. Rannacher, W. Wollner

Nr. 2011-20
November 2011

Computational Aspects of Pseudospectra in Hydrodynamic Stability Analysis

D. Gerecht[a], R. Rannacher[a,*], W. Wollner[b]

[a] *Institute of Applied Mathematics, University of Heidelberg, Im Neuenheimer Feld 293/294, D-69120 Heidelberg, Germany*
[b] *Department of Mathematics, University of Hamburg, Bundesstraße 55, D-20146 Hamburg, Germany*

Abstract

This paper addresses the analysis of spectra and pseudospectra of linearized Navier-Stokes operators from the numerical point of view. Pseudospectra play a crucial role in linear hydrodynamic stability theory and are closely related to the non-normality of the underlying differential operators and the matrices resulting from their discretization. This concept offers an explanation for experimentally observed instability in situations when eigenvalue-based linear stability analysis would predict stability. Hence the reliable numerical computation of pseudospectra is of practical importance particularly in situations when the stationary "base flow" is not analytically but only computationally given. The considered algorithm is based on a finite element discretization of the continuous eigenvalue problem and uses an Arnoldi-type method with a multigrid component. Its performance is investigated theoretically as well as practically at several two-dimensional test examples such as the linearized Burgers equations and various problems involving the Navier-Stokes equations for incompressible flow.

Keywords: Navier-Stokes equations, linearized stability, pseudospectrum, finite element method, Arnoldi method, non-normal operators

1. Introduction

This paper investigates an algorithm for analyzing spectra and pseudospectra of non-symmetric linear differential operators and discusses its performance from the numerical point of view. The pseudospectrum of a differential operator at a point $z \in \mathbb{C}$ determines the size of a perturbation of the operator, under which this point would become an eigenvalue of the perturbed operator. Consequently, the pseudospectrum serves as a mean to investigate the influence of perturbations on the eigenvalues of an operator. The concept of a pseudospectrum has been advocated in Trefethen [32, 33], and Trefethen & Embree

*Corresponding author

[34] in the context of non-normal matrices resulting from the discretization of certain non-symmetric differential operators. It has gained attention especially in hydrodynamic stability theory since it offers an explanation for certain well-known phenomena of experimentally observed instability in situations, when eigenvalue-based linear stability analysis would predict stability. In this case, the stability of a stationary solution to the nonlinear system is analyzed by studying the behavior of the associated linearized system, which is determined by the eigenvalues of the corresponding linearized operator.

For example, in two or three dimensions the classical Couette flow and Poiseuille flow are stationary solutions of the Navier-Stokes equations for any Reynolds number. In experiments these solutions turn nonstationary or even chaotic for higher Reynolds numbers depending on the experimental set up. However, linear stability analysis based on the eigenvalues of the corresponding linearized Navier-Stokes operator predicts stability for Couette flow for all Reynolds numbers and stability of Poiseuille flow for Reynolds numbers much larger than the critical ones observed in experiment. The reason of this failure of linear stability theory was found in the presence of a large pseudospectrum corresponding to small "stable" eigenvalues, which causes significant initial growth of small perturbations in the linearized system eventually triggering nonlinear instability. For a discussion of this aspect, we refer to Trefethen et al. [35] and Johnson et al. [19].

Hence the reliable numerical computation of pseudospectra is of practical importance particularly in situations when the stationary "base flow" is not analytically but only computationally given. Until now the computation of pseudospectra has been restricted to matrices of moderate size and therefore mainly to ordinary differential operators, such as the Orr-Sommerfeld operator as a simplified model for the full Navier-Stokes equations (see Trefethen et al. [36]). The goal of this paper is to analyze, theoretically as well as practically, a method for computing critical pseudospectra of the linearized Navier-Stokes operator even in cases when the stationary base flow is not known analytically. This method is based on a finite element discretization of the continuous eigenvalue problem and uses an Arnoldi-type method, such as proposed in Trefethen & Embree [34] and Trefethen [33]. For increasing efficiency the latter algorithm involves a multigrid component. For a similar approach to solving large nonsymmetric eigenvalue problems, we refer to Heuveline & Bertsch [13]. The adaptive finite element discretization of such problems has been treated in Heuveline & Rannacher [14] and Rannacher et al. [28]. The effectivity of the described method is illustrated by several test examples in two space dimensions such as the vector Burgers equation and the Navier-Stokes equations linearized around stationary "base solutions".

The following crucial questions are investigated in computing pseudospectra for the finite element analogue of the linearized Navier-Stokes operator:

1. For which choices of the various parameters in the numerical scheme are the computed pseudospectra reliable?
2. How sensitive are computed eigenvalues and pseudospectra with respect

to stabilization of pressure and transport in the numerical scheme?
3. Is it possible to detect the presence of a critical pseudospectrum a posteriori without explicitly computing it?
4. Do the computed pseudospectra of the discrete operators actually converge to that of the continuous one?
5. How does the pseudospectrum depend on the inflow and outflow boundary conditions imposed on admissible perturbations?
6. How do the pseudospectra of the linearized Burgers operator compare to that of the linearized Navier-Stokes operator?

All these questions have not been satisfactorily considered yet in the literature. The results presented in this paper are in some parts based on the Diploma theses Westenberger [37], see also Rannacher et al. [28], and Gerecht [10] and also use material from Heuveline & Rannacher [15] and Rannacher [27]

The content of the paper is as follows: In Section 2, we recall the basics of linear hydrodynamic stability theory, particularly the aspect of pseudospectra related to the non-normality of the underlying operators. Section 3 deals with the finite element method used in our computations and addresses the convergence of discrete pseudospectra. Section 4 presents our algorithm for computing eigenvalues and pseudospectra of matrices based on the Arnoldi method and singular value decomposition. Section 5 presents an application in stability analysis, for the vector Burgers equation linearized around a Couette-like solution. We especially address the effect of different inflow and outflow boundary conditions and of the various parameters in the solution algorithm on the structure and accuracy of the computed pseudospectra. Then, in Section 6, we investigate the analogous questions for the Navier-Stokes equations, at first for its linearization around Couette flow and Poiseuille flow, and finally for the stationary solution of a flow benchmark "channel flow around a cylinder". All numerical computations use the software package GASCOIGNE [9].

2. Stability analysis

In this section, we recall the concept of linear stability analysis and its shortcomings for non-normal operators. Further, we describe the finite element discretization of the Navier-Stokes equations in the common velocity-pressure formulation used in our computations.

Let $\Omega \subset \mathbb{R}^d$, $d = 2$ or $d = 3$, be a bounded domain with polygonal or polyhedral boundary $\partial\Omega$, respectively. We use the standard notation $L^2(\Omega)$, $H^1(\Omega)$, and $H_0^1(\Gamma;\Omega) = \{v \in H^1(\Omega) \mid v|_\Gamma = 0\}$, $\Gamma \subset \partial\Omega$, for the Lebesgue and Sobolev spaces on Ω, with the corresponding norms denoted by $\|\cdot\|$ and $\|\cdot\|_m$, respectively. Occasionally also L^p and $W^{m,p}$ spaces for $1 \le p \le \infty$ and $m \in \mathbb{N}$ will be used together with the corresponding notation of norms. Spaces of $\mathbb{R}^d$-valued functions $v = (v_1, \ldots, v_d)$ are denoted by boldface-type, but no distinction is made in the notation of norms and inner products, e.g., $\mathbf{L}^2(\Omega) = L^2(\Omega)^d$ and $\mathbf{H}_0^1(\Gamma;\Omega) = H_0^1(\Gamma;\Omega)^d$ have norm $\|\cdot\| = (\sum_{i=1}^d \|v_i\|^2)^{1/2}$

and $\|v\|_1 = (\sum_{i=1}^d \|v_i\|_1^2)^{1/2}$, respectively. All other notation is self-evident, e.g., $\partial_t u = \partial u/\partial t$ and $\partial_n v = n \cdot \nabla v$, where n is an outer normal unit vector.

We assume a decomposition $\partial\Omega = \Gamma_{\text{in}} \cup \Gamma_{\text{out}} \cup \Gamma_{\text{rigid}}$, where Γ_{in}, Γ_{out}, and Γ_{rigid} denote the inlet, the outlet and the rigid part of the boundary $\partial\Omega$, respectively. We introduce the abbreviations $L := L^2(\Omega)$, $\mathbf{L} := L(\Omega)^d$, and

$$\hat{\mathbf{H}} := \mathbf{H}^1(\Omega), \quad \hat{\mathbf{V}} := \hat{\mathbf{H}} \times L, \qquad \mathbf{H} := \mathbf{H}_0^1(\Gamma_{\text{in}} \cup \Gamma_{\text{rigid}}, \Omega), \quad \mathbf{V} := \mathbf{H} \times L.$$

In the case $\Gamma_{\text{out}} = \emptyset$, we use $L := L_0^2(\Omega) = \{q \in L^2(\Omega) | \, (q,1) = 0\}$. For theoretical analysis it is convenient to introduce spaces of solenoidal functions in order to eliminate the pressure from the discussion (see, e.g., Galdi [8]),

$$\mathbf{J}_1 := \{v \in \mathbf{H}, \, \nabla \cdot v = 0\}, \qquad \mathbf{J}_0 := \overline{\mathbf{J_1}}^{\|\cdot\|} \subset \mathbf{L}.$$

In this context let $\tilde{P}$ denote the so-called "Stokes projection", i.e., the orthogonal projection of $\mathbf{L}$ onto its subspace $\mathbf{J}_0$.

With this notation, we consider the following eigenvalue problem occurring in hydrodynamic stability theory:

$$\begin{aligned} &-\nu\Delta v + \hat{v} \cdot \nabla v + v \cdot \nabla \hat{v} + \nabla q = \lambda v, \quad \nabla \cdot v = 0, \quad \text{in } \Omega, \\ &v|_{\Gamma_{\text{rigid}} \cup \Gamma_{\text{in}}} = 0, \;\; \nu\partial_n v - qn|_{\Gamma_{\text{out}}} = 0. \end{aligned} \tag{1}$$

Here, the pair $\{\hat{v}, \hat{p}\}$ is a stationary "base flow", i.e., a stationary solution of the corresponding Navier-Stokes equations

$$\begin{aligned} &-\nu\Delta \hat{v} + \hat{v} \cdot \nabla \hat{v} + \nabla \hat{p} = f, \quad \nabla \cdot \hat{v} = 0, \quad \text{in } \Omega, \\ &\hat{v}|_{\Gamma_{\text{rigid}}} = 0, \;\; \hat{v}|_{\Gamma_{\text{in}}} = v^{\text{in}}, \;\; \nu\partial_n \hat{v} - \hat{p}n|_{\Gamma_{\text{out}}} = P, \end{aligned} \tag{2}$$

where $\hat{v}$ is the velocity vector field of the flow, $\hat{p}$ its hydrostatic pressure, and ν the kinematic viscosity (for normalized density $\rho \equiv 1$). The flow is driven by a prescribed flow velocity v^{in} at the Dirichlet (inflow) boundary, a mean pressure P at the Neumann (outflow) boundary, and a volume force f. The (artificial) "free outflow" (also called "do nothing") boundary condition in (1) and (2) has proven successful especially in modeling pipe flow since it is satisfied by Poiseuille flow (see Heywood et al. [16]).

The goal is to investigate the stability of the base flow under small perturbations, which leads us to consider the eigenvalue problem (1). If an eigenvalue $\lambda \in \mathbb{C}$ of (1) has $\operatorname{Re}\lambda < 0$, the base flow is unstable, otherwise it is said to be "linearly stable". This means that the solution of the linearized nonstationary perturbation problem

$$\begin{aligned} &\partial_t w - \nu\Delta w + \hat{v} \cdot \nabla w + w \cdot \nabla \hat{v} + \nabla q = 0, \quad \nabla \cdot w = 0, \quad \text{in } \Omega, \\ &w|_{\Gamma_{\text{rigid}} \cup \Gamma_{\text{in}}} = 0, \quad \nu\partial_n w - qn|_{\Gamma_{\text{out}}} = 0 \end{aligned} \tag{3}$$

corresponding to an initial perturbation $w_{|t=0} = w_0$ satisfies a bound

$$\sup_{t \geq 0} \|w(t)\| \leq A\|w_0\|, \tag{4}$$

for some constant $A \geq 1$. However, "linear stability" does not guarantee full "nonlinear stability" due to effects caused by the "non-normality" of the operator governing problem (1), which may cause the constant A to become large. This is related to the possible "deficiency" (discrepancy of geometric and algebraic multiplicity) or a large "pseudo-spectrum" (range of large resolvent norm) of the critical eigenvalue. This effect is commonly accepted as explanation of the discrepancy in the stability properties of simple base flows such as Couette flow and Poiseuille flow predicted by linear eigenvalue-based stability analysis and experimental observation. Indeed, Fourier analysis shows that for Couette flow at all Reynolds numbers the relevant eigenvalues have positive real part and for Poiseuille they are like this up to Reynolds number $\mathrm{Re} \approx 5772$. However, for both flows in the experiment transition to chaotic behavior happens for much smaller Reynolds numbers depending on the experimental setup (see, e.g., Trefethen & Embree [34] and Trefethen et al. [36], and the literature cited therein).

2.1. Stability analysis in a variational setting

For pairs $\{v,p\},\{\varphi,\chi\} \in \hat{\mathbf{V}}$, we define the semilinear form

$$a(v;\varphi) := \nu(\nabla v,\nabla\varphi) + (v\cdot\nabla v,\varphi),$$

the bilinear form $b(p,\varphi) := -(p,\nabla\cdot\varphi)$, and the functional $F(\varphi) := (f,\varphi) + (Pn,\varphi)_{\Gamma_{\mathrm{out}}}$. With a solenoidal extension $\bar{v}^{\mathrm{in}} \in \hat{\mathbf{H}}$ of the inflow data v^{in}, we consider a solution $\{\hat{v},\hat{p}\} \in \mathbf{V}+\{\bar{v}^{\mathrm{in}},0\}$ of the saddle point problem

$$a(\hat{v};\varphi) + b(\hat{p},\varphi) - b(\chi,\hat{v}) = F(\varphi) \quad \forall\{\varphi,\chi\} \in \mathbf{V}. \tag{5}$$

This "base solution" $\{\hat{v},\hat{p}\}$ shall be (locally) unique. Further, we assume that the derivative form

$$a'(\hat{v};\psi,\varphi) := \nu(\nabla\psi,\nabla\varphi) + (\hat{v}\cdot\nabla\psi,\varphi) + (\psi\cdot\nabla\hat{v},\varphi)$$

is regular on $\mathbf{H}$, i.e., it satisfies the stability condition

$$\inf_{\psi\in\mathbf{H}}\Big\{\sup_{\varphi\in\mathbf{H}}\frac{a'(\hat{v};\psi,\varphi)}{\|\nabla\varphi\|\|\nabla\psi\|}\Big\} \geq \gamma > 0.$$

This means that $\lambda = 0$ is not an eigenvalue of (1). A corresponding "inf-sup" condition is known to hold for the pressure form,

$$\inf_{p\in L}\Big\{\sup_{\varphi\in\mathbf{H}}\frac{b(p,\varphi)}{\|\nabla\varphi\|\|p\|}\Big\} \geq \beta > 0.$$

The associated linearized stability analysis considers the following nonstationary linearized perturbation equation for $v = v(t) \in \mathbf{J}_1$:

$$(\partial_t v,\varphi) + a'(\hat{v};v,\varphi) = 0 \quad \forall\varphi \in \mathbf{J}_1, \tag{6}$$

with the initial condition $v(0) = v_0 \in \mathbf{J}_0$. The stability of $\hat{v}$ under "small" perturbations is then characterized by the growth property of the corresponding solution operator $S(t) : \mathbf{J}_0 \to \mathbf{J}_0$, $v(t) = S(t)v_0$,

$$\|S(t)\| \approx Ae^{-\mathrm{Re}\lambda\, t}, \quad t \geq 0, \tag{7}$$

where $A \geq 1$ and λ is a most critical eigenvalue, i.e., one with smallest real part, of the stability eigenvalue problem

$$-\nu\Delta v + \hat{v} \cdot \nabla v + v \cdot \nabla \hat{v} + \nabla q = \lambda v, \quad \nabla \cdot v = 0. \tag{8}$$

If one of the eigenvalues has negative real part, then the base solution $\hat{v}$ is unstable. The variational formulation of this eigenvalue problem reads

$$a'(\hat{v}; v, \varphi) = \lambda\,(v, \varphi) \quad \forall \varphi \in \mathbf{J}_1, \tag{9}$$

with the normalization $\|v\| = 1$. Using the operators $\mathcal{A}(\hat{v}) := \tilde{P}(-\nu\Delta\hat{v}+\hat{v}\cdot\nabla\hat{v})$ and $\mathcal{A}'(\hat{v})v := \tilde{P}(-\nu\Delta v + \hat{v} \cdot \nabla v + v \cdot \nabla\hat{v})$, the eigenvalue problem (9) reads in operator notation like $\mathcal{A}'(\hat{v})v = \lambda\mathcal{I}v$. Since the domain Ω is bounded, the resolvent $\mathcal{A}'(\hat{v})^{-1}$ is a compact operator and the classical Riesz-Schauder theory applies (see Kato [20]). Accordingly, the eigenvalue problem (9) possesses a countably infinite set $\Sigma(\mathcal{A}'(\hat{v})) := \{\lambda_i\}_{i=1}^{\infty} \subset \mathbb{C}$ of isolated eigenvalues with finite (algebraic) multiplicities which have no finite accumulation points. The difference between the algebraic and geometric multiplicity of an eigenvalue λ, its so-called "defect", is denoted by $\alpha \in \mathbb{N}_0$ and corresponds to the largest integer such that $\ker((\mathcal{A}'(\hat{v}) - \lambda\mathcal{I})^{\alpha+1}) \neq \ker((\mathcal{A}'(\hat{v}) - \lambda\mathcal{I})^{\alpha})$. Associated to a primal eigenfunction $v \in \mathbf{J}_1$, there is a "dual" (left) eigenfunction $v^* \in \mathbf{J}_1\backslash\{0\}$ corresponding to λ, that is determined by the "dual" eigenvalue problem

$$a'(\hat{v}; \varphi, v^*) = \lambda\,(\varphi, v^*) \quad \forall \varphi \in \mathbf{J}_1, \tag{10}$$

or $\mathcal{A}'(\hat{v})^* v^* = \lambda^* \mathcal{I} v^*$ in operator notation. Here, $\lambda^* = \bar{\lambda}$ and the dual eigenfunction may also be normalized to $\|v^*\| = 1$ or to $(v, v^*) = 1$, if $\alpha = 0$ and λ is simple. In the degenerate case $(v, v^*) = 0$, then (and only then) the problem

$$a'(\hat{v}; v^1, \varphi) - \lambda\,(v^1, \varphi) = (v, \varphi) \quad \forall \varphi \in \mathbf{J}_1, \tag{11}$$

possesses a solution $v^1 \in \mathbf{J}_1$, a "generalized eigenfunction" with $(v^1, v) = 0$. In this case the eigenvalue λ has defect $\alpha \geq 1$ and the solution operator $S(t)$ has the growth property

$$\|S(t)\| \approx t^{\alpha} e^{-\mathrm{Re}\lambda\, t}. \tag{12}$$

The effect of degeneracy on the numerical approximation of the Navier-Stokes equations has been addressed in Johnson et al. [19].

2.2. The effect of non-normality and the pseudospectrum

The existence of an eigenvalue with $\mathrm{Re}\lambda < 0$ inevitably causes dynamic instability of the base flow $\hat{v}$, i.e., arbitrarily small perturbations may grow without bound. This is induced by the growth property

$$\|S(t)\| \approx t^{\alpha} e^{-\mathrm{Re}\lambda\, t} \to \infty \quad (t \to \infty). \tag{13}$$

However, even for $0 < \mathrm{Re}\lambda \ll 1$ the property (13) of $S(t)$ implies

$$\sup_{t>0} \|S(t)\| \approx \Big(\frac{\alpha}{e}\Big)^{\alpha} \frac{1}{|\mathrm{Re}\lambda|^{\alpha}}, \tag{14}$$

i.e., small perturbations may initially be amplified to an extent such that nonlinear instability occurs. Therefore, we are mainly interested in the case that all eigenvalues have positive real part and want to compute the most "critical" eigenvalues, that is those λ with minimal $\mathrm{Re}\lambda > 0$. The crucial question is how to detect computationally whether the growth factor in the estimate (13) may become critical or not.

However, a similar effect is also possible for non-deficient eigenvalues λ. This is related to the concept of the "pseudo-spectrum" described in Trefethen [32], Trefethen & Embree [34] and the literature cited therein. For $\varepsilon \in \mathbb{R}_+$ the ε-pseudo-spectrum $\Sigma_\varepsilon(\mathcal{A}) \subset \mathbb{C}$ of the operator $\mathcal{A} := \mathcal{A}'(\hat{v})$ in the Hilbert space $\mathbf{J}_0$ is defined by

$$\Sigma_\varepsilon(\mathcal{A}) := \big\{ z \in \mathbb{C} \setminus \Sigma(\mathcal{A}) \big|\ \|(\mathcal{A} - z\mathcal{I})^{-1}\| \geq \varepsilon^{-1} \big\} \cup \Sigma(\mathcal{A}), \tag{15}$$

where $\|\cdot\|$ denotes the natural operator norm.

Remark 2.1. The "pseudospectrum" is interesting only for non-normal operators, since for a normal operator $\Sigma_\varepsilon(\mathcal{A})$ is just the union of ε-circles around its eigenvalues. This follows from the estimate (see Dunford & Schwartz [5] or Kato [20])

$$\|(z\mathcal{I} - \mathcal{A})^{-1}\| \geq \mathrm{dist}(z, \Sigma(\mathcal{A}))^{-1}, \quad z \notin \Sigma(\mathcal{A}), \tag{16}$$

where equality holds if $\mathcal{A}$ is normal.

The concept of "pseudospectrum" can be introduced for closed linear operators in abstract Hilbert or Banach spaces (see Trefethen & Embree [34]). Typically hydrodynamic stability analysis concerns differential operators defined on bounded domains. This situation fits into the Hilbert-space framework of "closed unbounded operators with compact inverse". Here, we use this approach for the special case of operators generated by sesquilinear forms on (complex) Hilbert spaces.

Let V, H be two abstract complex (separable) Hilbert space with scalar products and corresponding norms denoted by $(\cdot,\cdot)_V$, $(\cdot,\cdot) = (\cdot,\cdot)_H$ and $\|\cdot\|_V$, $\|\cdot\| = \|\cdot\|_H$, respectively, which form a so-called Gelfand triple, $V \subset H \subset V^*$, where V^* is the (complex) dual of V. The embedding $V \subset H$ is assumed to

be dense and compact. Typical examples relevant for the subject of this paper are the Gelfand triples $H_0^1(\Gamma;\Omega) \subset L^2(\Omega) \subset H^{-1}(\Gamma;\Omega)$ and $\mathbf{J}_1 \subset \mathbf{J}_0 \subset \mathbf{J}_1^*$. On V, we consider a sesquilinear form $a(\cdot,\cdot)$, which is assumed to be bounded,

$$|a(u,v)| \leq \alpha \|u\|_V \|v\|_V, \quad u,v \in V, \tag{17}$$

and to satisfy a Garding's inequality,

$$a(v,v) \in \mathbb{R}, \quad a(v,v) + \gamma\|v\|^2 \geq \beta \|v\|_V^2, \quad v \in V, \tag{18}$$

with certain constants $\beta > 0$ and $\gamma \geq 0$. Without loss of generality, for the following, we assume that the sesquilinear form $a(\cdot,\cdot)$ is "coercive", i.e., (18) holds with $\gamma = 0$. In this case, by the Lax-Milgram lemma, for any $f \in H$ there exists a unique solution $u \in V$ of the variational equations

$$a(u,\varphi) = (f,\varphi)_H, \quad \forall \varphi \in V. \tag{19}$$

Then, the sesquilinear form $a(\cdot,\cdot)$ generates an (abstract) operator $\mathcal{A} : D(\mathcal{A}) \subset V \subset H \to H$ (not to be confused with the linearized Navier-Stokes operator from above) by

$$(\mathcal{A}v,\varphi)_H := a(v,\varphi), \quad v \in D(\mathcal{A}),\ \varphi \in V,$$

where

$$D(\mathcal{A}) = \big\{ v \in V \big|\ |a(v,\varphi)| \leq c(v)\|\varphi\|,\ \varphi \in H \big\}.$$

This operator is densely defined and onto, and its inverse $\mathcal{A}^{-1}$ viewed as a mapping $\mathcal{A}^{-1} : H \to D(\mathcal{A}) \subset H$ is compact. The operator $\mathcal{A}$ with compact inverse is "closed", i.e., its graph in $D(\mathcal{A}) \times H$ is closed. The space of such densely defined closed linear operators is denoted by $\mathcal{C}(H)$ and the space of all bounded linear operators on H by $\mathcal{B}(H)$. By construction the eigenvalue problem of the operator $\mathcal{A}$ is equivalent to the variational eigenvalue problem

$$a(v,\varphi) = \lambda(v,\varphi) \quad \forall \varphi \in V, \tag{20}$$

and, if $0 \notin \Sigma(\mathcal{A})$, to the eigenvalue problem of the inverse,

$$\mathcal{A}^{-1}v = \lambda^{-1}v. \tag{21}$$

Remark 2.2. Since we only consider operators defined in Hilbert spaces, we can alternatively use weak or strict inequality signs in the definition (15) of the pseudospectrum without changing its properties. This may be different in the context of operators in Banach spaces without inner product; for a discussion of this problem see Trefethen & Embree [34]

The first part of the following lemma can be found in in Trefethen & Embree [34]. For completeness, we recall a sketch of the argument.

Lemma 2.1. *(i) For an operator $\mathcal{A} \in \mathcal{C}(H)$ the following definitions of the ε-pseudospectrum are equivalent:*

(a) $\Sigma_\varepsilon(\mathcal{A}) := \big\{z \in \mathbb{C} \setminus \Sigma(\mathcal{A}) \big| \ \|(\mathcal{A} - z\mathcal{I})^{-1}\| \geq \varepsilon^{-1}\big\} \cup \Sigma(\mathcal{A})$.

(b) $\Sigma_\varepsilon(\mathcal{A}) := \big\{z \in \mathbb{C} \big| \ z \in \Sigma(\mathcal{A} + \mathcal{E})$ *for some* $\mathcal{E} \in \mathcal{B}(H)$ *with* $\|\mathcal{E}\| \leq \varepsilon\big\}$.

(c) $\Sigma_\varepsilon(\mathcal{A}) := \big\{z \in \mathbb{C} \big| \ \|(\mathcal{A} - z\mathcal{I})v\| \leq \varepsilon$ *for some* $v \in D(\mathcal{A})$ *with* $\|v\| = 1\big\}$.

(ii) Let $0 \notin \Sigma(\mathcal{A})$. Then, the ε-pseudospectra of $\mathcal{A}$ and that of its inverse $\mathcal{A}^{-1} : H \to D(\mathcal{A}) \subset H$ are related by

$$\Sigma_\varepsilon(\mathcal{A}) \subset \big\{z \in \mathbb{C} \setminus \{0\} \ \big| \ z^{-1} \in \Sigma_{\delta(z)}(\mathcal{A}^{-1})\big\} \cup \{0\}, \tag{22}$$

where $\delta(z) := \varepsilon\|\mathcal{A}^{-1}\|/|z|$ and, for $0 < \varepsilon < 1$, by

$$\Sigma_\varepsilon(\mathcal{A}^{-1}) \cap B_1(0)^c \subset \big\{z \in \mathbb{C} \setminus \{0\} \ \big| \ z^{-1} \in \Sigma_\delta(\mathcal{A})\big\}, \tag{23}$$

where $B_1(0) := \{z \in \mathbb{C},\ |z| \leq 1\}$ and $\delta := \varepsilon/(1 - \varepsilon)$.

Proof. (ia) In all three definitions, we have $\Sigma(\mathcal{A}) \subset \Sigma_\varepsilon(\mathcal{A})$. Let $z \in \Sigma_\varepsilon(\mathcal{A})$ in the sense of definition (a), there exists $w \in H$ with $\|w\| = 1$, such that $\|(\mathcal{A} - z\mathcal{I})^{-1}w\| \geq \varepsilon^{-1}$. Hence, there is a $v \in H$, $\|v\| = 1$, and $s \in (0, \varepsilon)$, such that $(\mathcal{A} - z\mathcal{I})^{-1}w = s^{-1}\mathcal{I}v$ or $(\mathcal{A} - z\mathcal{I})v = s\mathcal{I}w$. Let $\mathcal{Q}(v, w) \in \mathcal{B}(H)$ denote the unitary mapping, which rotates the unit vector v into the unit vector w, such that $s\mathcal{I}w = s\mathcal{Q}(v, w)v$. Then, $z \in \Sigma(\mathcal{A} + \mathcal{E})$ where $\mathcal{E} := s\mathcal{Q}(v, w)$ with $\|\mathcal{E}\| \leq \varepsilon$, i.e., $z \in \Sigma_\varepsilon(\mathcal{A})$ in the sense of definition (b). Let now be $z \in \Sigma_\varepsilon(\mathcal{A})$ in the sense of definition (b), i.e., there exists $\mathcal{E} \in \mathcal{B}(H)$ with $\|\mathcal{E}\| \leq \varepsilon$ such that $(\mathcal{A} + \mathcal{E})w = z\mathcal{I}w$, with some $w \in D(\mathcal{A})$, $w \neq 0$. Hence, $(\mathcal{A} - z\mathcal{I})w = -\mathcal{E}w$, and therefore,

$$\begin{aligned}
\|(\mathcal{A} - z\mathcal{I})^{-1}\| &= \sup_{v \in H} \frac{\|(\mathcal{A} - z\mathcal{I})^{-1}v\|}{\|v\|} = \sup_{v \in D(\mathcal{A})} \frac{\|v\|}{\|(\mathcal{A} - z\mathcal{I})v\|} \\
&= \Big(\inf_{v \in D(\mathcal{A})} \frac{\|(\mathcal{A} - z\mathcal{I})v\|}{\|v\|}\Big)^{-1} \geq \Big(\frac{\|(\mathcal{A} - z\mathcal{I})w\|}{\|w\|}\Big)^{-1} \\
&= \Big(\frac{\|\mathcal{E}w\|}{\|w\|}\Big)^{-1} \geq \|\mathcal{E}\|^{-1} \geq \varepsilon^{-1}.
\end{aligned}$$

Hence, $z \in \Sigma_\varepsilon(\mathcal{A})$ in the sense of definition (a). This proves the equivalence of definitions (a) and (b).

(ib) Next, let again $z \in \Sigma_\varepsilon(\mathcal{A}) \setminus \Sigma(\mathcal{A})$ in the sense of definition (a). Then,

$$\varepsilon \geq \|(\mathcal{A} - z\mathcal{I})^{-1}\|^{-1} = \Big(\sup_{w \in H} \frac{\|(\mathcal{A} - z\mathcal{I})^{-1}w\|}{\|w\|}\Big)^{-1} = \inf_{v \in D(\mathcal{A})} \frac{\|(\mathcal{A} - z\mathcal{I})v\|}{\|v\|}.$$

Hence, there exists a $v \in D(\mathcal{A})$ with $\|v\| = 1$, such that $\|(\mathcal{A} - z\mathcal{I})v\| \leq \varepsilon$, i.e., $z \in \Sigma_\varepsilon(\mathcal{A})$ in the sense of definition (c). By the same argument, now used in the reversed direction, we see that $z \in \Sigma_\varepsilon(\mathcal{A})$ in the sense of definition (c)

implies that also $z \in \Sigma_\varepsilon(\mathcal{A})$ in the sense of definition (a). Thus, definition (a) is also equivalent to condition (c).

(iia) We use the definition (c) from part (i) for the ε-pseudospectrum. Let $z \in \Sigma_\varepsilon(\mathcal{A})$ and accordingly $v \in D(\mathcal{A})$, $\|v\| = 1$, satisfying $\|(\mathcal{A} - z\mathcal{I})v\| \le \varepsilon$. Then,

$$\|(\mathcal{A}^{-1} - z^{-1}\mathcal{I})v\| = \|z^{-1}\mathcal{A}^{-1}(z\mathcal{I} - \mathcal{A})v)\| \le |z|^{-1}\|\mathcal{A}^{-1}\|\varepsilon.$$

This proofs the asserted relation (22).

(iib) To prove the relation (23), we again use the definition (c) from part (i) for the ε-pseudospectrum. Accordingly, for $z \in \Sigma_\varepsilon(\mathcal{A}^{-1})$ with $|z| \ge 1$ there exists a unit vector $v \in \mathbf{H}$, $\|v\| = 1$, such that

$$\varepsilon \ge \|(z\mathcal{I} - \mathcal{A}^{-1})v\| = |z|\|(\mathcal{A} - z^{-1}\mathcal{I})\mathcal{A}^{-1}v\|.$$

Hence, setting $w := \|\mathcal{A}^{-1}v\|^{-1}\mathcal{A}^{-1}v \in D(\mathcal{A})$ with $\|w\| = 1$, we obtain

$$\|(\mathcal{A} - z^{-1}\mathcal{I})w\| \le |z|^{-1}\|\mathcal{A}^{-1}v\|^{-1}\varepsilon.$$

Hence, observing that

$$\|\mathcal{A}^{-1}v\| = \|(\mathcal{A}^{-1} - z\mathcal{I})v + zv\| \ge \|zv\| - \|(\mathcal{A}^{-1} - z\mathcal{I})v\| \ge |z| - \varepsilon,$$

we conclude that

$$\|(\mathcal{A} - z^{-1}\mathcal{I})w\| \le \frac{\varepsilon}{|z|(|z| - \varepsilon)} \le \frac{\varepsilon}{1 - \varepsilon}.$$

This completes the proof. □

2.3. Pseudospectrum and stability analysis

Now, we turn back to the concrete situation of hydrodynamic stability analysis. First, we recall a result on the possible size of the amplification constant A in the stability estimate (7), which in the finite dimensional case is referred to as the "easy half" of the "Kreiss matrix theorem" (see Kreiss [21] and Trefethen & Embree [34] and the references cited therein). In the case of a stationary base solution this estimate can easily be obtained by employing the Laplace transform for semigroups (see Trefethen et al. [35]). Here, we supply an elementary argument, which could also be used in the case of a *quasi-stationary* base solution.

Lemma 2.2. *Let $\mathcal{A} := \mathcal{A}'(\hat{v})$ and $z \in \mathbb{C} \setminus \Sigma(\mathcal{A})$ with $\mathrm{Re}z < 0$. Then, for the solution operator $S(t) : \mathbf{J}_0 \to \mathbf{J}_0$ of the linear perturbation equation (9), there holds*

$$\sup_{t \ge 0} \|S(t)\| \ge |\mathrm{Re}z|\,\|(\mathcal{A} - z\mathcal{I})^{-1}\| \tag{24}$$

and, consequently, in terms of the pseudospectrum

$$\sup_{t \ge 0} \|S(t)\| \ge \sup\big\{|\mathrm{Re}z|\varepsilon^{-1} \mid \varepsilon > 0, z \in \Sigma_\varepsilon(\mathcal{A}), \mathrm{Re}z < 0\big\}. \tag{25}$$

Proof. For $z \notin \Sigma(\mathcal{A})$, the inverse $(\mathcal{A} - zI)^{-1}$ is well defined as a bounded operator in $\mathbf{J}_0$. Let $w_0 := w|_{t=0} \in \mathbf{J}_0$, be an arbitrary but nontrivial initial perturbation. We recall that $w(t) = S(t)w_0$. We rewrite the perturbation equation (3) in strong form

$$\partial_t w + zw + (\mathcal{A} - zI)w = 0,$$

and multiply by e^{tz}, to obtain

$$\partial_t(e^{tz}w) + e^{tz}(\mathcal{A} - zI)w = 0.$$

Next, integrating this over $0 \le t < \infty$ and observing $\mathrm{Re}z < 0$ yields

$$(\mathcal{A} - zI)^{-1}w_0 = \int_0^\infty e^{tz}S(t)\,dt\,w_0.$$

From this, we conclude

$$\|(\mathcal{A} - zI)^{-1}\| \le |\mathrm{Re}z|^{-1} \sup_{t>0} \|S(t)\|,$$

which implies the asserted estimate. □

The next proposition relates the size of the resolvent norm $\|(\mathcal{A}'(\hat{v}) - z\mathcal{I})^{-1}\|$ to easily computable quantities in terms of the eigenvalues and eigenfunctions of the operator $\mathcal{A}'(\hat{v})$. The proof is recalled from Heuveline & Rannacher [15].

Theorem 2.1. *Let $\lambda \in \mathbb{C}$ be a non-deficient eigenvalue of the operator $\mathcal{A} := \mathcal{A}'(\hat{v})$ with corresponding primal and dual eigenvectors $v, v^* \in \mathbf{J}_1$ normalized by $\|v\| = (v, v^*) = 1$. Then, there exists a continuous function $\omega : \mathbb{R}_+ \to \mathbb{C}$ with $\lim_{\varepsilon \searrow 0+} \omega(\varepsilon) = 1$, such that for $\lambda_\varepsilon := \lambda - \varepsilon\omega(\varepsilon)\|v^*\|$, there holds*

$$\|(\mathcal{A} - \lambda_\varepsilon\mathcal{I})^{-1}\| \ge \varepsilon^{-1}, \tag{26}$$

i.e., the point λ_ε lies in the ε-pseudospectrum of the operator $\mathcal{A}$.

Proof. (i) Let $b(\cdot,\cdot)$ be a continuous bilinear form on $\mathbf{J}_0$, such that

$$\sup_{\psi,\varphi \in \mathbf{J}_1} \frac{|b(\psi,\varphi)|}{\|\psi\|\,\|\varphi\|} \le 1.$$

We consider the perturbed eigenvalue problem, for $\varepsilon \in \mathbb{R}_+$,

$$a'(\hat{v}; v_\varepsilon, \varphi) + \varepsilon b(v_\varepsilon, \varphi) = \lambda_\varepsilon\,(v_\varepsilon, \varphi) \quad \forall \varphi \in \mathbf{J}_1. \tag{27}$$

Since this is a regular perturbation and λ non-deficient, there exist corresponding eigenvalues $\lambda_\varepsilon \in \mathbb{C}$ and eigenfunctions $v_\varepsilon \in \mathbf{J}_1$, $\|v_\varepsilon\| = 1$, such that

$$|\lambda_\varepsilon - \lambda| = \mathcal{O}(\varepsilon), \quad \|v_\varepsilon - v\| = \mathcal{O}(\varepsilon).$$

Furthermore, from the relation

$$a'(\hat{v}; v_\varepsilon, \varphi) - \lambda_\varepsilon(v_\varepsilon, \varphi) = -\varepsilon b(v_\varepsilon, \varphi), \quad \varphi \in \mathbf{J}_1,$$

we conclude that

$$\sup_{\varphi\in\mathbf{J}_1}\frac{|a'(\hat v;v_\varepsilon,\varphi)-\lambda_\varepsilon(v_\varepsilon,\varphi)|}{\|\varphi\|}\le\varepsilon\sup_{\varphi\in\mathbf{J}_1}\frac{|b(v_\varepsilon,\varphi)|}{\|\varphi\|}\le\varepsilon\,\|v_\varepsilon\|,$$

and from this, if λ_ε is not an eigenvalue of $\mathcal{A}$,

$$\|(\mathcal{A}-\lambda_\varepsilon\mathcal{I})^{-1}\|^{-1}=\inf_{\psi\in\mathbf{J}_1}\sup_{\varphi\in\mathbf{J}_1}\frac{|a'(\hat v;\psi,\varphi)-\lambda_\varepsilon(\psi,\varphi)|}{\|\psi\|\,\|\varphi\|}\le\varepsilon.$$

This implies the asserted estimate

$$\|(\mathcal{A}-\lambda_\varepsilon\mathcal{I})^{-1}\|\ge\varepsilon^{-1}. \tag{28}$$

(ii) Next, we analyze the dependence of the eigenvalue λ_ε on ε in more detail. Subtracting the equation for v from that for v_ε, we obtain

$$a'(\hat v;v_\varepsilon-v,\varphi)+\varepsilon b(v_\varepsilon,\varphi)=(\lambda_\varepsilon-\lambda)(v_\varepsilon,\varphi)+\lambda(v_\varepsilon-v,\varphi).$$

Taking $\varphi=v^*$ yields

$$a'(\hat v;v_\varepsilon-v,v^*)+\varepsilon b(v_\varepsilon,v^*)=(\lambda_\varepsilon-\lambda)(v_\varepsilon,v^*)+\lambda(v_\varepsilon-v,v^*)$$

and, using the equation satisfied by v^*,

$$\varepsilon b(v_\varepsilon,v^*)=(\lambda_\varepsilon-\lambda)(v_\varepsilon,v^*).$$

This yields $\lambda_\varepsilon=\lambda+\varepsilon\omega(\varepsilon)b(v,v^*)$, where, observing $v_\varepsilon\to v$ and $(v,v^*)=1$,

$$\omega(\varepsilon):=\frac{b(v_\varepsilon,v^*)}{(v_\varepsilon,v^*)b(v,v^*)}\to1\quad(\varepsilon\to0).$$

(iii) It remains to construct an appropriate perturbation form $b(\cdot,\cdot)$. For convenience, we consider the renormalized dual eigenfunction $\tilde v^*:=v^*\|v^*\|^{-1}$, satisfying $\|\tilde v^*\|=1$. With the function $w:=(v-\tilde v^*)\|v-\tilde v^*\|^{-1}$, we set for $\varphi,\psi\in\mathbf{J}_0$

$$S\psi:=\psi-2\mathrm{Re}(\psi,w)w,\qquad b(\psi,\varphi):=-(S\psi,\varphi).$$

The operator $S:\mathbf{J}_0\to\mathbf{J}_0$ acts like a Householder transformation mapping v into $\tilde v^*$. In fact, observing $\|v\|=\|\tilde v^*\|=1$, there holds

$$\begin{aligned}Sv&=v-\frac{2\mathrm{Re}(v,v-\tilde v^*)}{\|v-\tilde v^*\|^2}(v-\tilde v^*)=\frac{(2-2\mathrm{Re}(v,\tilde v^*))v-2\mathrm{Re}(v,v-\tilde v^*)(v-\tilde v^*)}{2-2\mathrm{Re}(v,\tilde v^*)}\\&=\frac{2v-2\mathrm{Re}(v,\tilde v^*)v-2v+2\mathrm{Re}(v,\tilde v^*)v+(2-2\mathrm{Re}(v,\tilde v^*))\tilde v^*}{2-2\mathrm{Re}(v,\tilde v^*)}=\tilde v^*.\end{aligned}$$

This implies that

$$b(v,v^*)=-(Sv,v^*)=-(\tilde v^*,v^*)=-\|v^*\|.$$

Further, observing $\|w\| = 1$ and

$$\|Sv\|^2 = \|v\|^2 - 2\mathrm{Re}(v,w)(v,w) - 2\mathrm{Re}(v,w)(w,v) + 4\mathrm{Re}(v,w)^2\|w\|^2 = \|v\|^2,$$

we have

$$\sup_{v,\varphi\in\mathbf{J}_1} \frac{|b(v,\varphi)|}{\|v\|\,\|\varphi\|} \le \sup_{v,\varphi\in\mathbf{J}_1} \frac{\|Sv\|\,\|\varphi\|}{\|v\|\,\|\varphi\|} = 1.$$

Hence, for this particular choice of the form $b(\cdot,\cdot)$, we have

$$\lambda_\varepsilon = \lambda - \varepsilon\omega(\varepsilon)\|v^*\|, \qquad \lim_{\varepsilon\to 0}\omega(\varepsilon) = 1,$$

as asserted. □

Remark 2.3. (i) We note that the statement of Theorem 2.1 becomes trivial if the operator $\mathcal{A} := \mathcal{A}'(\hat{v})$ is *normal*. In this case primal and dual eigenvectors coincide and, in view of Remark 2.1, $\Sigma_\varepsilon(\mathcal{A})$ is the union of ε-circles around its eigenvalues λ. Hence, observing $\|v^*\| = \|v\| = 1$ and setting $\omega(\varepsilon) \equiv 1$, we trivially have $\lambda_\varepsilon := \lambda - \varepsilon \in \Sigma_\varepsilon(\mathcal{A})$ as asserted.

(ii) If $\mathcal{A}$ is nonnormal it may have a nontrivial pseudospectrum. Then, a large norm of the dual eigenfunction $\|v^*\|$ corresponding to a critical eigenvalue λ_{crit} with $0 < \mathrm{Re}\lambda_{\mathrm{crit}} \ll 1$, indicates that the ε-pseudospectrum $\Sigma_\varepsilon(\mathcal{A})$, even for small ε, reaches into the left complex half plane.

(iii) If the eigenvalue $\lambda \in \Sigma(\mathcal{A})$ considered in Theorem 2.1 is deficient, the normalization $(v, v^*) = 1$ is not possible. In this case, as discussed above, there is another mechanism for triggering nonlinear instability.

2.3.1. The deficiency test

The result of Theorem 2.1 may be used in hydrodynamic stability analysis as follows: Suppose that the spectrum of the linearized Navier-Stokes operator $\mathcal{A} := \mathcal{A}'(\hat{v})$ lies in the positive complex half-plane and let λ_{crit} be its (non-deficient) eigenvalue with smallest real part, $0 < \mathrm{Re}\lambda_{\mathrm{crit}} \ll 1$. Further, let v and v^* be associated eigenfunctions normalized for instance by $\|v\| = (v, v^*) = 1$. Then, in view of Remark 2.3 (ii), a large value $\|v^*\| \gg 1$ indicates a possibly large growth constant A. The statement of Theorem 2.1 ensures that for any $\varepsilon \in \mathbb{R}_+$ for which $\lambda_\varepsilon := \lambda_{\mathrm{crit}} - \varepsilon\omega(\varepsilon)\|v^*\|$ satisfies

$$\mathrm{Re}\lambda_\varepsilon = \mathrm{Re}\lambda_{\mathrm{crit}} - \varepsilon\mathrm{Re}\omega(\varepsilon)\|v^*\| < 0, \tag{29}$$

there holds $\lambda_\varepsilon \in \Sigma_\varepsilon(\mathcal{A})$. Consequently, by Lemma 2.2,

$$\sup_{t\ge 0}\|S(t)\| \ge |\mathrm{Re}\lambda_\varepsilon|\,\|(\mathcal{A} - \lambda_\varepsilon\mathcal{I})^{-1}\| \ge \frac{|\mathrm{Re}\lambda_\varepsilon|}{\varepsilon}. \tag{30}$$

For small ε, we may set $\omega(\varepsilon) = 1$. Hence, taking for example $\varepsilon = 2\mathrm{Re}\lambda_{\mathrm{crit}}\|v^*\|^{-1}$, it follows that $\mathrm{Re}\lambda_\varepsilon \approx -\mathrm{Re}\lambda_{\mathrm{crit}} < 0$, and consequently,

$$\sup_{t\ge 0}\|S(t)\| \ge \tfrac{1}{2}\|v^*\|. \tag{31}$$

In order to computationally test the validity of the predicted relation $\lambda_\varepsilon \in \Sigma_\varepsilon(\mathcal{A})$, we may choose $\varepsilon = 2\mathrm{Re}\lambda_{\mathrm{crit}}\|v^*\|^{-1} \ll \mathrm{Re}\lambda_{\mathrm{crit}}$ as proposed above and check, whether for

$$\lambda_\varepsilon := \lambda_{\mathrm{crit}} - \varepsilon\|v^*\| = \lambda_{\mathrm{crit}} - 2\mathrm{Re}\lambda_{\mathrm{crit}}, \quad \mathrm{Re}\lambda_\varepsilon = -\mathrm{Re}\lambda_{\mathrm{crit}} < 0,$$

there holds $\lambda_\varepsilon \in \Sigma_\varepsilon(\mathcal{A})$.

3. The Galerkin finite element approximation

The discretization of the variational problem (5) and of its associated eigenvalue problem uses a standard second-order finite element method as described, for instance, in Girault & Raviart [12], Quarteroni & Valli [24], and Rannacher [25, 26]. Let $\mathbb{T}_h$ be decompositions of $\overline{\Omega}$ into cells K (closed triangles, quadrilaterals, etc.). The local width of a cell $K \in \mathbb{T}_h$ is $h_K := \mathrm{diam}(K)$, while $h := \max_{K\in\mathbb{T}_h} h_K$ denotes the global mesh size. For simplicity, we consider here only low-order tensor-product elements, that is piecewise d-linear trial and test functions for all unknowns (so-called equal-order "Q_1/Q_1 Stokes element"). In order to ease local mesh refinement and coarsening, we allow "hanging" nodes where the corresponding "irregular" nodal values are eliminated from the system by linear interpolation of neighboring regular nodal values, see Figure 1. The corresponding finite element subspaces are denoted by $L_h \subset L$ and

$$\hat{\mathbf{H}}_h \subset \hat{\mathbf{H}}, \quad \mathbf{H}_h \subset \mathbf{H}, \qquad \hat{\mathbf{V}}_h := \hat{\mathbf{H}}_h \times L_h, \quad \mathbf{V}_h := \mathbf{H}_h \times L_h.$$

Here, we assume the domain Ω to be polygonal such that the boundary $\partial\Omega$ can be exactly matched by the mesh domain $\overline{\Omega}_h := \cup\{K \in \mathbb{T}_h\}$. In the case of a curved boundary certain modifications are necessary, which are rather standard in finite element analysis (see Ciarlet [4]).

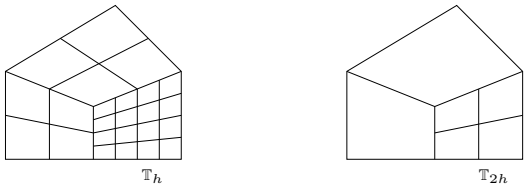

Figure 1: Two-dimensional mesh $\mathbb{T}_h$ (with hanging nodes) organized in a patchwise manner with corresponding coarser mesh $\mathbb{T}_{2h}$.

Since the finite element approximations $v_h \in \mathbf{H}_h$ of $v \in \mathbf{J}_1$ are usually not exactly solenoidal, we have to include the approximate pressures $p_h \in L_h$ in the analysis. Therefore, from now on we will consider approximating pairs $\{v_h, p_h\} \in \mathbf{V}_h$ to $\{v, p\} \in \mathbf{V}$. Further, for notational simplification, we introduce the spaces of discretely solenoidal functions

$$\mathbf{J}_h := \big\{v_h \in \mathbf{H}_h \big|\ (\chi_h, \nabla\cdot v_h) = 0 \ \ \forall \chi_h \in L_h\big\},$$

but $\mathbf{J}_h \not\subset \mathbf{J}_1$ in general. In order to obtain a stable discretization in these spaces with "equal-order interpolation" of pressure and velocity, we use a reduced version of the "Galerkin Least-Squares Stabilization" (GLS) of Hughes et al. [18] or the "Local Projection Stabilization" (LPS) of Becker & Braack [1]. By the same techniques, we also obtain the stabilization of the transport in case of dominant advection. In this case the GLS stabilization is closely related to the "Streamline Upwinding Petrov-Galerkin Stabilization" (SUPG) of Hughes & Brooks [17].

3.1. Stabilized "equal-order" discretization of the Navier-Stokes problem

First, we describe two common stabilization techniques in solving the Navier-Stokes equations to obtain the base solution. The GLS uses the mesh-dependent inner product and norm

$$(\varphi,\psi)_h := \sum\nolimits_{K\in\mathbb{T}_h} (\varphi,\psi)_K, \quad \|\varphi\|_h = (\varphi,\varphi)_h^{1/2},$$

for defining the following stabilizing form, for pairs $\{v_h,q_h\},\{\varphi_h,\chi_h\} \in \hat{\mathbf{V}}_h$:

$$s_h(\{v_h,q_h\};\{\varphi_h,\chi_h\}) := \big(v_h\cdot\nabla v_h + \nabla q_h, \delta_h v_h\cdot\nabla\varphi_h + \alpha_h\nabla\chi_h\big)_h,$$

with mesh-dependent parameters $\delta_h|_K = \delta_K$ and $\alpha_h|_K = \alpha_K$. Then, the stabilized discrete Navier-Stokes problem seeks $\{\hat{v}_h,\hat{p}_h\} \in \mathbf{V}_h + \{\bar{v}_h^{\mathrm{in}},0\}$, such that

$$a(\hat{v}_h;\varphi_h) + s_h(\{\hat{v}_h,\hat{p}_h\};\{\varphi_h,\chi_h\}) + b(\hat{p}_h,\varphi_h) - b(\chi_h,\hat{v}_h) = F(\varphi_h), \qquad (32)$$

for all $\{\varphi_h,\chi_h\} \in \mathbf{V}_h$, where $\bar{v}_h^{\mathrm{in}} \in \mathbf{J}_h$ is a suitable approximation of the inflow data v^{in}. The stabilization parameters are chosen according to $\alpha_K = \alpha_0\gamma_K$ and $\delta_K = \delta_0\gamma_K$, where

$$\gamma_K := \min\Big(\frac{h_K^2}{6\nu}, \frac{h_K}{\|v_h\|_K}\Big), \quad K\in\mathbb{T}_h,$$

and usually $\alpha_0 = \delta_0 = 0.3$ (see Franca et al. [7]). Though this discretization is not "strongly" consistent, i.e., the stabilization does not vanish at the continuous solution, it preserves the optimal order of the discretization. The LPS applies stabilization only to the scale of the finest mesh $\mathbb{T}_h$ by using a local projection or interpolation operator $\pi_{2h} : \mathbf{V}_h \to \mathbf{V}_{2h}$ to the next coarser mesh $\mathbb{T}_{2h}$. The stabilizing form is then defined by

$$\begin{aligned} s_h(\{v_h,q_h\};\{\varphi_h,\chi_h\}) := {} & \big(v_h\cdot\nabla(v_h-\pi_{2h}v_h), \delta_h v_h\cdot\nabla(\varphi_h-\pi_{2h}\varphi_h)\big)_h \\ & + \big(\nabla(q_h-\pi_{2h}q_h), \alpha_h\nabla(\chi_h-\pi_{2h}\chi_h)\big)_h, \end{aligned}$$

with the stabilization parameters α_k and δ_K as specified above. For the economical realization of the projection π_{2h}, we use hierarchically block-structured meshes such as shown in Figure 1. The LPS is also not strongly consistent but preserves the total order of convergence of the discretization. It also results in augmented discrete problems of the form (32). We note that problem (32) cannot be simplified by eliminating the pressure through reducing it to the subspace $\mathbf{J}_h$ of "solenoidal" functions since the stabilization also acts on the pressure variable.

3.2. "Inf-sup"-stable discretization of the Navier-Stokes boundary value problem

Most of the numerical results presented in this paper have been obtained using the stabilized equal-order Q_1/Q_1 Stokes element described above. But at some places also the Q_2/Q_1 Taylor-Hood element is employed (see Quarteroni & Valli [24] or Rannacher [25]). This Stokes element uses continuous biquadratic shape functions for the velocity and bilinear ones for the pressure. It is inf-sup-stable, e.g., it holds

$$\inf_{q_h \in L_h} \left\{ \sup_{\varphi_h \in \mathbf{H}_h} \frac{b(\varphi_h, q_h)}{\|\varphi_h\|_1} \right\} \geq \beta' > 0, \tag{33}$$

and therefore does not require extra pressure stabilization. It is mainly used in comparison to the Q_1/Q_1 Stokes element in order to rule out any negative effect on the computation of eigenvalues and pseudospectra possibly caused by the pressure stabilization. However, also this Stokes element requires transport stabilization in the case of higher Reynolds numbers. The corresponding stabilization forms are in the GLS approach

$$s_h(v_h; \varphi_h) := \big(v_h \cdot \nabla v_h, \delta_h v_h \cdot \nabla \varphi_h\big)_h,$$

and in the LPS approach

$$s_h(v_h; \varphi_h) := \big(v_h \cdot \nabla (v_h - \pi_{2h} v_h), \delta_h v_h \cdot \nabla (\varphi_h - \pi_{2h} \varphi_h)\big)_h.$$

3.3. Discretization of the Navier-Stokes eigenvalue problem

Next, we describe the discretization of the eigenvalue problem associated to the Navier-Stokes operator linearized around the stationary base solution $\{\hat{v}, \hat{p}\}$. In the case of the "equal-order" Stokes elements the definition of the stabilization by the GLS or LPS methods follows the same ideas as used for the nonlinear boundary value problem. For brevity, we now only consider the case of the "inf-sup"-stable Taylor-Hood element using GLS transport stabilization:

$$s_h(\hat{v}_h; v_h, \varphi_h) := \big(\hat{v}_h \cdot \nabla v_h, \delta_h \hat{v}_h \cdot \nabla \varphi_h\big)_h.$$

Then, the stabilized primal and dual discrete eigenvalue problems seek $\{v_h, q_h\}$ and $\{v_h^*, q_h^*\}$ in $\mathbf{V} \backslash \{0\}$ and $\lambda_h, \lambda_h^* \in \mathbb{C}$, such that

$$a'(\hat{v}_h; v_h, \varphi_h) + s_h(\hat{v}_h; v_h, \varphi_h) + b(q_h, \varphi_h) - b(\chi_h, v_h) = \lambda_h \, (v_h, \varphi_h), \tag{34}$$

$$a'(\hat{v}_h; \varphi_h, v_h^*) + s_h(\hat{v}_h; \varphi_h, v_h^*) + b(q_h^*, \varphi_h) - b(\chi_h, v_h^*) = \lambda_h^* \, (\varphi_h, v_h^*), \tag{35}$$

for all $\{\varphi_h, \chi_h\} \in \mathbf{V}_h$. The eigenfunctions are usually normalized by $\|v_h\| = \|v_h^*\| = 1$.

In the following, for conceptional simplicity, we will skip the transport stabilization in the formulation of the approximate eigenvalue problems. This is justified since all results stated for $h \to 0$ are of asymptotic nature. It allows us to state the approximate eigenvalue problems in the compact form

$$a'(\hat{v}_h; v_h, \varphi_h) = \lambda_h \, (v_h, \varphi_h) \quad \forall \varphi_h \in \mathbf{J}_h, \tag{36}$$

$$a'(\hat{v}_h; \varphi_h, v_h^*) = \lambda_h^* \, (\varphi_h, v_h^*) \quad \forall \varphi_h \in \mathbf{J}_h. \tag{37}$$

For the described Galerkin finite element discretizations, we can recall *a priori* error estimates from the literature. If the problem is H^2-regular, there holds an optimal-order L^2-error estimate for the approximation of the base solution (see Girault & Raviart [12] or Rannacher [25]),

$$\|\hat{v}_h - \hat{v}\| + h\|\nabla(\hat{v}_h - \hat{v})\| \;=\; \mathcal{O}(h^2), \tag{38}$$

and for a non-deficient eigenvalue (see Bramble & Osborn [2] and Osborn [23]),

$$|\lambda_h - \lambda| \;=\; \mathcal{O}(h^2). \tag{39}$$

Further, for pairs of normalized discrete primal and dual eigenfunctions $\{v_h, v_h^*\} \in \mathbf{J}_h \times \mathbf{J}_h$, there exists an associated pair of eigenfunctions $\{v^h, v^{h*}\} \in \mathbf{J}_1 \times \mathbf{J}_1$, such that

$$\|v_h - v^h\| + \|v_h^* - v^{h*}\| \;=\; \mathcal{O}(h^2). \tag{40}$$

Here, the superscript in v^h indicates that the continuous eigenfunction associated to v_h may vary with h.

Remark 3.1. In the case that problem (2) is H^2-regular and that the data is sufficiently smooth, then in addition to the L^2-error estimate (38) there also hold L^p-error estimates

$$\|\hat{v}_h - \hat{v}\|_{L^p} \;=\; \mathcal{O}(h^2|\ln(h)|^{\omega(p)}), \tag{41}$$

where $2 \le p \le \infty$ with $\omega(p) = 0$ for $2 \le p < \infty$, and $\omega(\infty) = 1$. For proofs of such results, we refer to Duran & Nochetto [6], Girault et al. [11], Chen [3], and the literature cited therein. In case that problem (2) is not H^2-regular, for instance if the domain Ω has reentrant corners, then the above convergence orders are reduced to $\mathcal{O}(h^\alpha)$ for some $\alpha \in [1, 2)$.

Remark 3.2. The above asymptotic error estimates are usually proven in the literature for the special case $\Gamma_{\text{out}} = \emptyset$ only. In this situation the relation

$$(\psi \cdot \nabla v, \varphi) = ((\nabla \cdot \psi)v, \varphi) - (\psi \cdot \nabla\varphi, v), \quad \psi, \varphi, v \in \mathbf{H}, \tag{42}$$

holds true since integration by parts does not produce any boundary term. This significantly simplifies the argument but the generalization to the case $\Gamma_{\text{out}} \neq \emptyset$ only requires standard arguments in estimating the additional boundary term $((n \cdot \psi)v, \varphi)_{\Gamma_{\text{out}}}$. However, in the following, our analysis will take care of this possible complication since the case of free in- or outflow turns out to be the most interesting one in the stability analysis. At one point, we like to use the error estimate

$$|(\varphi\psi, \hat{v}_h - \hat{v})_{\Gamma_{\text{out}}}| \le ch^2\|\varphi\|_1\|\psi\|_1, \quad \varphi, \psi \in \mathbf{H}^1(\Omega), \tag{43}$$

which, in view of (41), is likely to hold true, but for which we unfortunately cannot give a reference. However, a corresponding estimate with order $\mathcal{O}(h^{2-\varepsilon})$, for any $\varepsilon \in (0, 1)$ can be derived from the error estimates (41) by using standard trace theorems.

Now, let $z \notin \Sigma(\mathcal{A}'(\hat{v}))$ be a regular point and $w \in \mathbf{J}_1$ be the (unique) solution of the variational problem

$$a'_z(\hat{v}; w, \varphi) := a'(\hat{v}; w, \varphi) - z(w, \varphi) = (f, \varphi) \quad \forall \varphi \in \mathbf{J}_1, \tag{44}$$

for some right hand side $f \in \mathbf{J}_0$. Assume that (5) is H^2-regular, than this linear boundary value problem is H^2-regular, i.e., its solution is in $\mathbf{H}^2(\Omega)$ and there holds the a priori estimate

$$\|w\|_2 \le c(\hat{v}, z)\|f\|, \tag{45}$$

where the constant $c(\hat{v}, z)$ depends on $\operatorname{dist}(z, \Sigma(\mathcal{A}'(\hat{v}))^{-1}$.

Lemma 3.1. *Suppose that problem (2) is H^2-regular and that the error estimates (38), (41), and (43) hold true. Then, if $z \notin \Sigma(\mathcal{A}'(\hat{v}))$, for sufficiently small h, z is also a regular point for the discrete equations*

$$a'_z(\hat{v}_h; w_h, \varphi_h) = (f, \varphi_h) \quad \forall \varphi_h \in \mathbf{J}_h. \tag{46}$$

For the corresponding solutions $w_h \in \mathbf{J}_h$ there holds the error estimate

$$\|w_h - w\| + h\|\nabla(w_h - w)\| \le c(\hat{v}, z)h^2\|f\|. \tag{47}$$

Proof. (i) The assumption $z \notin \Sigma(\mathcal{A}'(\hat{v}))$ implies that

$$\sup_{\varphi \in \mathbf{H}} \frac{a'_z(\hat{v}; \psi, \varphi)}{\|\varphi\|_1} \ge \gamma(\hat{v}, z)\|\psi\|_1, \quad \psi \in \mathbf{H}. \tag{48}$$

For $\varphi \in \mathbf{H}$ let $i_h\varphi \in \mathbf{H}_h$ an H^1-stable interpolation satisfying

$$\|\varphi - i_h\varphi\| + h\|\nabla i_h\varphi\| \le ch\|\varphi\|_1.$$

For such a construction, we refer to Scott & Zhang [31]. Then, with this notation,

$$\begin{aligned}
\gamma(\hat{v}, z)\|\psi_h\|_1 &\le \sup_{\varphi \in \mathbf{H}} \frac{a'_z(\hat{v}; \psi_h, \varphi)}{\|\varphi\|_1} \\
&\le \sup_{\varphi \in \mathbf{H}} \frac{a'_z(\hat{v}; \psi_h, \varphi - i_h\varphi)}{\|\varphi\|_1} + \sup_{\varphi \in \mathbf{H}} \frac{a'_z(\hat{v}; \psi_h, i_h\varphi)}{\|i_h\varphi\|_1} \frac{\|i_h\varphi\|_1}{\|\varphi\|_1} \\
&\le \sup_{\varphi \in \mathbf{H}} \frac{a'_z(\hat{v}; \psi_h, \varphi - i_h\varphi)}{\|\varphi\|_1} + c \sup_{\varphi_h \in \mathbf{H}_h} \frac{a'_z(\hat{v}; \psi_h, \varphi_h)}{\|\varphi_h\|_1} \\
&\le c\|\psi_h\|_1\|\hat{v}\|_2 \sup_{\varphi \in \mathbf{H}} \frac{\|\varphi - i_h\varphi\|}{\|\varphi\|_1} + c \sup_{\varphi_h \in \mathbf{H}_h} \frac{a'_z(\hat{v}; \psi_h, \varphi_h)}{\|\varphi_h\|_1} \\
&\le c(\hat{v})h\|\psi_h\|_1 + c \sup_{\varphi_h \in \mathbf{H}_h} \frac{a'_z(\hat{v}; \psi_h, \varphi_h)}{\|\varphi_h\|_1},
\end{aligned}$$

and consequently,

$$(\gamma(\hat{v}, z) - c(\hat{v})h)\|\psi_h\|_1 \le c \sup_{\varphi_h \in \mathbf{H}_h} \frac{a'_z(\hat{v}; \psi_h, \varphi_h)}{\|\varphi_h\|_1}. \tag{49}$$

Using the usual Sobolev inequalities and the estimate (38), we obtain

$$\begin{aligned} a_z'(\hat{v}_h;\psi_h,\varphi_h) &= a_z'(\hat{v};\psi_h,\varphi_h) + ((\hat{v}_h-\hat{v})\cdot\nabla\psi_h,\varphi_h) + (\psi_h\cdot\nabla(\hat{v}_h-\hat{v}),\varphi_h) \\ &\le a_z'(\hat{v};\psi_h,\varphi_h) + 2\|\hat{v}_h-\hat{v}\|_1\|\psi_h\|_1\|\varphi_h\|_1 \\ &\le a_z'(\hat{v};\psi_h,\varphi_h) + c(\hat{v})h\|\psi_h\|_1\|\varphi_h\|_1. \end{aligned}$$

Combining this with (49), we conclude

$$\sup_{\varphi_h\in\mathbf{H}_h} \frac{a_z'(\hat{v}_h;\psi_h,\varphi_h)}{\|\varphi_h\|_1} \ge (\gamma(\hat{v},z) - c(\hat{v})h)\|\psi_h\|_1, \tag{50}$$

which proves the first assertion.

(ii) Next, we consider the solution $\tilde{w}_h \in \mathbf{J}_h$ of the discrete intermediate problem

$$a_z'(\hat{v};\tilde{w}_h,\varphi_h) = (f,\varphi_h) \quad \forall\varphi_h \in \mathbf{J}_h. \tag{51}$$

This is the standard finite element approximation to the solution $w \in \mathbf{J}_1$ of (44) defined through the same bilinear form $a_z'(\hat{v};\cdot,\cdot)$. For this, we can recall the error estimate

$$\|\tilde{w}_h - w\| + h\|\nabla(\tilde{w}_h - w)\| \le c(\hat{v},z)h^2\|f\| \tag{52}$$

from the literature (see Girault & Raviart [12] or Rannacher [25]). Particularly, there holds

$$\|\tilde{w}_h\|_1 \le \|\tilde{w}_h - w\|_1 + \|w\|_1 \le c(\hat{v},z)\|f\|. \tag{53}$$

We note that the corresponding error estimate for the associated pressures is not needed here.

(iii) It remains to estimate the difference $e_h := w_h - \tilde{w}_h$. Comparing the corresponding equations, we find that for any $\varphi_h \in \mathbf{J}_h$ there holds

$$\begin{aligned} a_z'(\hat{v};e_h,\varphi_h) &= a_z'(\hat{v};w_h,\varphi_h) - a_z'(\hat{v};\tilde{w}_h,\varphi_h) + a_z'(\hat{v}_h;w_h,\varphi_h) - a_z'(\hat{v}_h;w_h,\varphi_h) \\ &= a_z'(\hat{v};w_h,\varphi_h) - a_z'(\hat{v}_h;w_h,\varphi_h) \\ &= ((\hat{v}-\hat{v}_h)\cdot\nabla w_h,\varphi_h) + (w_h\cdot\nabla(\hat{v}-\hat{v}_h),\varphi_h) \\ &= ((\hat{v}-\hat{v}_h)\cdot\nabla w_h,\varphi_h) - (w_h\cdot\nabla\varphi_h,\hat{v}-\hat{v}_h) \\ &\quad - ((\nabla\cdot w_h)\varphi_h,\hat{v}-\hat{v}_h) + ((n\cdot w_h)\varphi_h,\hat{v}-\hat{v}_h)_{\Gamma_{\rm out}}. \end{aligned}$$

Then, using the Sobolev embedding inequalities together with the error estimates (41) and (43) yields

$$\begin{aligned} |a_z'(\hat{v};e_h,\varphi_h)| &\le \|\hat{v}-\hat{v}_h\|_{L^3}\|\nabla w_h\|_{L^2}\|\varphi_h\|_{L^6} + \|w_h\|_{L^6}\|\nabla\varphi_h\|_{L^2}\|\hat{v}-\hat{v}_h\|_{L^3} \\ &\quad + \|\nabla w_h\|_{L^2}\|\varphi_h\|_{L^6}\|\hat{v}-\hat{v}_h\|_{L^3} + |((n\cdot w_h)\varphi_h,\hat{v}-\hat{v}_h)_{\Gamma_{\rm out}}| \\ &\le c(\hat{v},z)h^2\|w_h\|_1\|\varphi_h\|_1. \end{aligned}$$

Using this in the stability estimate (48) with $\psi := e_h$, we obtain

$$\begin{aligned}\|e_h\|_1 &\le \gamma(\hat v,z)^{-1}\sup_{\varphi\in\mathbf{H}}\frac{a_z'(\hat v;e_h,\varphi)}{\|\varphi\|_1}\\ &\le \gamma(\hat v,z)^{-1}c(\hat v,z)h^2\|w_h\|_1 \le \gamma(\hat v,z)^{-1}c(\hat v,z)h^2\{\|e_h\|_1+\|\tilde w_h\|_1\}.\end{aligned}$$

Consequently, recalling the estimates (52) and (53), we conclude that for sufficiently small $h>0$:

$$\|e_h\|_1 \le c(\hat v,z)h^2\|f\|. \tag{54}$$

This together with (52) implies the asserted error estimate (47). □

3.4. Convergence of pseudospectra

Next, we study the approximation of the pseudospectrum of the linearized Navier-Stokes operator by those of its discrete finite element analogues.

The discrete variational equation (46) defines a linear operator denoted by $\mathcal{A}_h'(\hat v_h):\mathbf{J}_h\to\mathbf{J}_h$, which is considered as the discrete analog of $\mathcal{A}'(\hat v): D(\mathcal{A}'(\hat v))\subset\mathbf{J}_0\to\mathbf{J}_0$. In the following, we use the abbreviations $\mathcal{A}:=\mathcal{A}'(\hat v)$, $\mathcal{A}_z:=\mathcal{A}'(\hat v)-z\mathcal{I}$, and $\mathcal{A}_h:=\mathcal{A}_h'(\hat v_h)$, $\mathcal{A}_{h,z}:=\mathcal{A}_h'(\hat v_h)-z\mathcal{I}_h$. Further, we denote by $\tilde P$ and $\tilde P_h$ the L^2 projections onto $\mathbf{J}_0$ and $\mathbf{J}_h$, respectively. For $z\notin\Sigma(\mathcal{A}(\hat v))$, in terms of the corresponding solution operators $\mathcal{T}_z:=\mathcal{A}_z^{-1}\tilde P:\mathbf{H}\to\mathbf{J}_1\subset\mathbf{H}$ and $\mathcal{T}_{h,z}:=\mathcal{A}_{h,z}^{-1}\tilde P_h:\mathbf{H}_h\to\mathbf{J}_h\subset\mathbf{H}$, defined by $v=\mathcal{T}_z f$ and $v_h=\mathcal{T}_{h,z}f$, respectively, the L^2 error estimate (47) can be expressed in the form of convergence in the operator norm:

$$\|\mathcal{T}_{h,z}-\mathcal{T}_z\|\le c_*(\hat v,z)h^2. \tag{55}$$

Here, both operators $\mathcal{T}_z$ and $\mathcal{T}_{h,z}$ are considered as operators in $\mathbf{H}$. In case of reduced regularity of the problem, e.g., due to the presence of corner singularities, the estimate (55) holds with possibly reduced order $\mathcal{O}(h^\alpha)$ with some $\alpha\in[1,2)$. We make the following assumption.

Assumption 3.1. *(i) All eigenvalues of the linearized Navier-Stokes operator have positive real parts, i.e.,* $\Sigma(\mathcal{A}'(\hat v))\subset\mathbb{C}_+:=\{z\in\mathbb{C},\ \mathrm{Re}z>0\}$. *Then, by the result of Lemma 3.1, for sufficiently small* h, *also* $\Sigma(\mathcal{A}_h'(\hat v))\subset\mathbb{C}_+$.
(ii) For some suitable $\zeta\in\mathbb{C}_-:=\{z\in\mathbb{C},\ \mathrm{Re}z\le 0\}$ *the error estimate (55) holds uniformly for* $z\in\mathbb{C}_-+\zeta$, *i.e.,*

$$\|\mathcal{T}_{h,z+\zeta}-\mathcal{T}_{z+\zeta}\|\le c_*h^2,\quad z\in\mathbb{C}_-, \tag{56}$$

with a fixed constant $c_*:=c_*(\hat v,\zeta)$.

This assumption seems generic in the context of hydrodynamic stability theory, since here we are mainly interested in the critical case that the spectrum is contained in the right complex half-plane (suggesting stability) but with a pseudospectrum reaching into the left complex half-plane (causing instability). The assumption above states in particular that for given ϵ the ϵ-pseudospectrum does not reach arbitrarily far into the negative half-plane.

Lemma 3.2. *Let Assumption 3.1 be satisfied. Then, the pseudospectra of the discrete operators $\mathcal{T}_h$ converge to that of the continuous operator $\mathcal{T}$ in the sense that, for sufficiently small $h > 0$,*

$$\Sigma_{\varepsilon - c_* h^2}(\mathcal{T}_h) \cap \mathbb{C}_- \subset \Sigma_\varepsilon(\mathcal{T}) \cap \mathbb{C}_- \subset \Sigma_{\varepsilon + c_* h^2}(\mathcal{T}_h) \cap \mathbb{C}_-. \tag{57}$$

Proof. We note that for $z, \zeta \in \mathbb{C}$

$$z \in \Sigma_\varepsilon(\mathcal{T}) \;\Leftrightarrow\; z + \zeta \in \Sigma_\varepsilon(\mathcal{T}_\zeta), \qquad z \in \Sigma_\varepsilon(\mathcal{T}_h) \;\Leftrightarrow\; z + \zeta \in \Sigma_\varepsilon(\mathcal{T}_{h,\zeta}). \tag{58}$$

Let now $z \in \mathbb{C}_-$ and $\zeta \in C_-$ be given as in Assumption 3.1. In particular $z + \zeta \notin \Sigma(\mathcal{T}_{h,\zeta})$ and $z + \zeta \notin \Sigma(\mathcal{T}_\zeta)$.
(i) Let $z + \zeta \in \Sigma_\varepsilon(\mathcal{T}_{h,\zeta})$. We note the identity

$$(\mathcal{T}_\zeta - z\mathcal{I})^{-1} = (\mathcal{T}_{h,\zeta} - z\mathcal{I})^{-1} + (\mathcal{T}_\zeta - z\mathcal{I})^{-1}\big(\mathcal{T}_{h,\zeta} - \mathcal{T}_\zeta\big)(\mathcal{T}_{h,\zeta} - z\mathcal{I})^{-1}.$$

From this, we infer that

$$\|(\mathcal{T}_\zeta - z\mathcal{I})^{-1}\| \le \|\big(\mathcal{I} + (\mathcal{T}_\zeta - z\mathcal{I})^{-1}(\mathcal{T}_{h,\zeta} - \mathcal{T}_\zeta)\big)\| \|(\mathcal{T}_{h,\zeta} - z\mathcal{I})^{-1}\|,$$

and, consequently, by (56) with $z = 0$,

$$\|(\mathcal{T}_{h,\zeta} - z\mathcal{I})^{-1}\| \ge \frac{\|(\mathcal{T}_\zeta - z\mathcal{I})^{-1}\|}{1 + \|(\mathcal{T}_\zeta - z\mathcal{I})^{-1}\| \|\mathcal{T}_{h,\zeta} - \mathcal{T}_\zeta\|} \ge \frac{\|(\mathcal{T}_\zeta - z\mathcal{I})^{-1}\|}{1 + \|(\mathcal{T}_\zeta - z\mathcal{I})^{-1}\| c_* h^2}.$$

Since the function $\psi(x) = x(1 + c_* h^2 x)^{-1}$ is strictly increasing on $\mathbb{R}_+$, we conclude that, for $\|(\mathcal{T}_\zeta - z\mathcal{I})^{-1}\| \ge \varepsilon^{-1}$,

$$\|(\mathcal{T}_{h,\zeta} - z\mathcal{I})^{-1}\| \ge \frac{\varepsilon^{-1}}{1 + c_* h^2 \varepsilon^{-1}} = (\varepsilon + c_* h^2)^{-1}.$$

(ii) In the same way exchanging the role of $\mathcal{T}_{h,\zeta}$ and $\mathcal{T}_\zeta$, we conclude that, for $\|(\mathcal{T}_{h,\zeta} - z\mathcal{I})^{-1}\| > (\varepsilon - c_* h^2)^{-1}$,

$$\|(\mathcal{T}_\zeta - z\mathcal{I})^{-1}\| \ge \frac{(\varepsilon - c_* h^2)^{-1}}{1 + c_* h^2 (\varepsilon - c_* h^2)^{-1}} = (\varepsilon - c_* h^2 + c_* h^2)^{-1} = \varepsilon^{-1}.$$

In view of (58), this implies the asserted relation (57). □

Lemma 3.3. *Let Assumption 3.1 be satisfied. Then, the pseudospectra of the discrete operators $\mathcal{A}_h$ converge to those of the continuous operator $\mathcal{A}$ in the sense that, for $\varepsilon(1 + c_* h^2) \le 1$,*

$$\Sigma_{\varepsilon(1 - c_* h^2)}(\mathcal{A}_h) \cap \mathbb{C}_- \;\subset\; \Sigma_\varepsilon(\mathcal{A}) \cap \mathbb{C}_- \;\subset\; \Sigma_{\varepsilon(1 + c_* h^2)}(\mathcal{A}_h) \cap \mathbb{C}_-. \tag{59}$$

Proof. We use the notation $\mathcal{A}_\zeta := \mathcal{A} - \zeta\mathcal{I}$ and $\mathcal{A}_{h,\zeta} := \mathcal{A}_h - \zeta\mathcal{I}$ and note that

$$z - \zeta \in \Sigma_\varepsilon(\mathcal{A}) \;\Leftrightarrow\; z \in \Sigma_\varepsilon(\mathcal{A}_\zeta), \qquad z - \zeta \in \Sigma_\varepsilon(\mathcal{A}_h) \;\Leftrightarrow\; z \in \Sigma_\varepsilon(\mathcal{A}_{h,\zeta}). \tag{60}$$

Let now $z \in \mathbb{C}_-$ and $\zeta \in C_-$ be given as in Assumption 3.1.

(i) Let $z+\zeta \in \Sigma_\varepsilon(\mathcal{A}) \cap \mathbb{C}_-$ and hence $z \in \Sigma_\varepsilon(\mathcal{A}_\zeta)$. Then, there exists some $v \in D(\mathcal{A})$, $\|v\|=1$, such that $\|(\mathcal{A}_\zeta - z\mathcal{I})v\| \le \varepsilon$. From this, we infer

$$\begin{aligned}\varepsilon &\ge \|(\mathcal{A}_\zeta - z\mathcal{I})v\| \ge \|\tilde{P}_h(\mathcal{A}_\zeta - z\mathcal{I})v\| \\ &= \|(\mathcal{A}_{h,\zeta} - z\mathcal{I})(\mathcal{A}_{h,\zeta} - z\mathcal{I}_h)^{-1}\tilde{P}_h(\mathcal{A}_\zeta - z\mathcal{I})v\| \\ &= \|(\mathcal{A}_{h,\zeta} - z\mathcal{I})w_h\|\|(\mathcal{A}_{h,\zeta} - z\mathcal{I}_h)^{-1}\tilde{P}_h(\mathcal{A}_\zeta - z\mathcal{I})v\|\end{aligned}$$

where

$$w_h := \frac{(\mathcal{A}_{h,\zeta} - z\mathcal{I})^{-1}\tilde{P}_h(\mathcal{A}_\zeta - z\mathcal{I})v}{\|(\mathcal{A}_{h,\zeta} - z\mathcal{I})^{-1}\tilde{P}_h(\mathcal{A}_\zeta - z\mathcal{I})v\|} \in \mathbf{J}_h, \quad \|w_h\| = 1.$$

Further, by (56), we conclude

$$\begin{aligned}&\|(\mathcal{A}_{h,\zeta} - z\mathcal{I}_h)^{-1}\tilde{P}_h(\mathcal{A}_\zeta - z\mathcal{I})v\| \\ &= \|((\mathcal{A}_{h,\zeta} - z\mathcal{I}_h)^{-1}\tilde{P}_h - (\mathcal{A}_\zeta - z\mathcal{I})^{-1})(\mathcal{A}_\zeta - z\mathcal{I})v + v\| \\ &\ge \|v\| - \|((\mathcal{A}_{h,\zeta} - z\mathcal{I}_h)^{-1}\tilde{P}_h - (\mathcal{A}_\zeta - z\mathcal{I})^{-1})(\mathcal{A}_\zeta - z\mathcal{I})v\| \\ &\ge 1 - \|(\mathcal{A}_{h,\zeta} - z\mathcal{I}_h)^{-1}\tilde{P}_h - (\mathcal{A}_\zeta - z\mathcal{I})^{-1}\tilde{P}\|\|(\mathcal{A}_\zeta - z\mathcal{I})v\| \\ &= 1 - \|\mathcal{T}_{h,\zeta+z} - \mathcal{T}_{\zeta+z}\|\|(\mathcal{A}_\zeta - z\mathcal{I})v\| \\ &\ge 1 - c_* h^2\varepsilon.\end{aligned}$$

This shows that, for $\varepsilon(1+c_*h^2) \le 1$,

$$\|(\mathcal{A}_{h,\zeta} - z\mathcal{I})w_h\| \le \frac{\varepsilon}{\|(\mathcal{A}_{h,\zeta} - z\mathcal{I})^{-1}(\mathcal{A}_\zeta - z\mathcal{I})v\|} \le \frac{\varepsilon}{1 - c_* h^2\varepsilon} \le (1 + c_* h^2)\varepsilon,$$

and, therefore,

$$z \in \Sigma_\delta(\mathcal{A}_{h,\zeta}), \quad \delta = (1 + c_* h^2)\varepsilon.$$

In view of (60), we obtain $z - \zeta \in \Sigma_\delta(\mathcal{A}_h)$.

(ii) Next, let $z - \zeta \in \Sigma_\delta(\mathcal{A}_h) \cap \mathbb{C}_-$ for $\delta = (1 - c_* h^2)\varepsilon$. Then, in view of (60), $z \in \Sigma_\delta(\mathcal{A}_{h,\zeta})$ and there exists some $v_h \in \mathbf{J}_h$, $\|v_h\| = 1$, such that $\|(\mathcal{A}_h - z\mathcal{I}_h)v_h\| \le \delta$. From this, we infer that

$$\begin{aligned}\delta &\ge \|(\mathcal{A}_{h,\zeta} - z\mathcal{I})v_h\| \ge \|\tilde{P}(\mathcal{A}_{h,\zeta} - z\mathcal{I})v_h\| \\ &= \|(\mathcal{A}_\zeta - z\mathcal{I})(\mathcal{A}_\zeta - z\mathcal{I})^{-1}\tilde{P}(\mathcal{A}_{h,\zeta} - z\mathcal{I})v_h\| \\ &= \|(\mathcal{A}_\zeta - z\mathcal{I})w\|\|(\mathcal{A}_\zeta - z\mathcal{I})^{-1}\tilde{P}(\mathcal{A}_{h,\zeta} - z\mathcal{I})v_h\|\end{aligned}$$

where

$$w := \frac{(\mathcal{A}_\zeta - z\mathcal{I})^{-1}\tilde{P}(\mathcal{A}_{h,\zeta} - z\mathcal{I}_h)v_h}{\|(\mathcal{A}_\zeta - z\mathcal{I})^{-1}\tilde{P}(\mathcal{A}_{h,\zeta} - z\mathcal{I})v_h\|} \in D(\mathcal{A}), \quad \|w\| = 1.$$

Further, by (56), we conclude

$$\begin{aligned}
&\|(\mathcal{A}_\zeta - z\mathcal{I})^{-1}\tilde{P}(\mathcal{A}_{h,\zeta} - z\mathcal{I})v_h\| \\
&= \|((\mathcal{A}_\zeta - z\mathcal{I})^{-1}\tilde{P} - (\mathcal{A}_{h,\zeta} - z\mathcal{I})^{-1})(\mathcal{A}_{h,\zeta} - z\mathcal{I})v_h + v_h\| \\
&\geq \|v_h\| - \|((\mathcal{A}_\zeta - z\mathcal{I})^{-1}\tilde{P} - (\mathcal{A}_{h,\zeta} - z\mathcal{I})^{-1})(\mathcal{A}_{h,\zeta} - z\mathcal{I})v_h\| \\
&\geq 1 - \|(\mathcal{A}_\zeta - z\mathcal{I})^{-1}\tilde{P} - (\mathcal{A}_{h,\zeta} - z\mathcal{I})^{-1}\tilde{P}_h\|\|(\mathcal{A}_{h,\zeta} - z\mathcal{I})v_h\| \\
&= 1 - \|\mathcal{T}_{\zeta+z} - \mathcal{T}_{h,\zeta+z}\|\|(\mathcal{A}_{h,\zeta} - z\mathcal{I})v_h\| \\
&\geq 1 - c_* h^2\delta.
\end{aligned}$$

This shows that, for $\varepsilon(1 + c_* h^2) \leq 1$,

$$\|(\mathcal{A}_\zeta - z\mathcal{I})w\| \leq \frac{\delta}{\|(\mathcal{A}_\zeta - z\mathcal{I})^{-1}\tilde{P}(\mathcal{A}_{h,\zeta} - z\mathcal{I})v_h\|} \leq \frac{\delta}{1 - c_* h^2\delta} \leq \varepsilon,$$

and, therefore $z \in \Sigma_\varepsilon(\mathcal{A}_\zeta)$ or, in view of (60), $z - \zeta \in \Sigma_\varepsilon(\mathcal{A})$. This implies $\Sigma_{\varepsilon(1-c_* h^2)}(\mathcal{A}_h) \subset \Sigma_\varepsilon(\mathcal{A})$, which completes the proof. □

4. The computation of matrix eigenvalues and pseudospectra

In the following, we will devise an algorithm for computing the pseudospectrum of the discretized operator $\mathcal{A}_h := \mathcal{A}_h'(\hat{v}_h) : \mathbf{J}_h \to \mathbf{J}_h$ respectively its inverse $\mathcal{A}_h^{-1}$. In fact, the direct computation of the ε-pseudospectra of the operator $\mathcal{A}_h$ is not feasible since it represents the discretization of an unbounded operator. One rather considers the inverse operator $\mathcal{A}_h^{-1}$, which approximates the bounded inverse $\mathcal{A}^{-1}$ and computes its "largest" (dominant) eigenvalues.

Let $\{\varphi_h^i,\, i = 1, \ldots, n_v := \dim\mathbf{H}_h\}$ and $\{\chi_h^j,\, j = 1, \ldots, n_p := \dim L_h\}$ be standard nodal bases of the finite element spaces $\mathbf{H}_h$ and L_h, respectively. The eigenvector $v_h \in \mathbf{H}_h$ and the corresponding pressure $q_h \in L_h$ possess expansions

$$v_h = \sum\nolimits_{i=1}^{n_v} v_h^i \varphi_h^i, \qquad q_h = \sum\nolimits_{j=1}^{n_p} q_h^j \chi_h^j,$$

with the vectors of expansion coefficients likewise denoted by $v_h = (v_h^i)_{i=1}^{n_v} \in \mathbb{C}^{n_v}$ and $q_h = (q_h^j)_{j=1}^{n_p} \in \mathbb{C}^{n_p}$, respectively. With this notation the discrete variational eigenvalue problem (34) is equivalent to the generalized algebraic eigenvalue problem

$$\begin{bmatrix} S_h & B_h \\ B_h^T & 0 \end{bmatrix} \begin{bmatrix} v_h \\ q_h \end{bmatrix} = \lambda_h \begin{bmatrix} M_h & 0 \\ 0 & 0 \end{bmatrix} \begin{bmatrix} v_h \\ q_h \end{bmatrix}, \tag{61}$$

with the so-called stiffness matrix S_h, gradient matrix B_h and mass matrix M_h defined by

$$S_h := \big(a'(\hat{v}_h; \varphi_h^j, \varphi_h^i)\big)_{i,j=1}^{n_v}, \quad B_h := \big((\chi_h^j, \nabla\cdot\varphi_h^i)\big)_{i,j=1}^{n_v,n_p}, \quad M_h := \big((\varphi_h^j, \varphi_h^i)\big)_{i,j=1}^{n_v}.$$

As mentioned above, we suppress terms stemming from pressure stabilization. The generalized eigenvalue problem (61) can equivalently be written in the form

$$\begin{bmatrix} M_h & 0 \\ 0 & 0 \end{bmatrix} \begin{bmatrix} S_h & B_h \\ B_h^T & 0 \end{bmatrix}^{-1} \begin{bmatrix} M_h & 0 \\ 0 & 0 \end{bmatrix} \begin{bmatrix} v_h \\ q_h \end{bmatrix} = \mu_h \begin{bmatrix} M_h & 0 \\ 0 & 0 \end{bmatrix} \begin{bmatrix} v_h \\ q_h \end{bmatrix}, \tag{62}$$

where $\mu_h = \lambda_h^{-1}$. Since the pressure q_h only plays the role of a silent variable (62) reduces to the standard eigenvalue problem

$$T_h v_h = \mu_h M_h v_h, \tag{63}$$

with the matrix $T_h \in \mathbb{R}^{n_v \times n_v}$ defined by

$$\begin{bmatrix} T_h & 0 \\ 0 & 0 \end{bmatrix} := \begin{bmatrix} M_h & 0 \\ 0 & 0 \end{bmatrix} \begin{bmatrix} S_h & B_h \\ B_h^T & 0 \end{bmatrix}^{-1} \begin{bmatrix} M_h & 0 \\ 0 & 0 \end{bmatrix}.$$

In the next step, we describe how the pseudospectrum of the matrix eigenvalue problem (63) may be computed.

The following lemma collects some useful facts, which particularly hold for pseudospectra of matrices. The proof can be found in Trefethen [33] and Trefethen & Embree [34]. Here and in the following, we skip the index h in the notation of the matrices.

Lemma 4.1. *(i) The ε-pseudospectrum of a matrix $T \in \mathbb{C}^{n\times n}$ can be equivalently defined in the following way:*

$$\Sigma_\varepsilon(T) := \{z \in \mathbb{C} \,|\, \Sigma_{\min}(zI - T) \le \varepsilon\}, \tag{64}$$

where $\Sigma_{\min}(T)$ denotes the smallest singular value of the matrix T, i.e., $\Sigma_{\min}(T) := \min\{|\lambda|^{1/2} |\, \lambda \in \Sigma(TT^*)\}$, with the adjoint T^* of T.

(ii) The pseudospectrum $\Sigma_\varepsilon(T)$ of a matrix $T \in \mathbb{C}^{n\times n}$ is invariant under orthonormal transformations, i.e., for any unitary matrix $Q \in \mathbb{C}^{n\times n}$ there holds

$$\Sigma_\varepsilon(T) = \Sigma_\varepsilon(Q^{-1}TQ). \tag{65}$$

In view of Lemma 2.1 and Lemma 4.1 there are several different though equivalent definitions of the ε-pseudospectrum $\Sigma_\varepsilon(T)$ of a matrix $T \in \mathbb{C}^{n\times n}$, which can be taken as starting point for the computation of pseudospectra (see Trefethen [33] and Trefethen & Embree [34]). Here, we use the definition of Lemma 4.1. Let $\Sigma_\varepsilon(T)$ to be determined in a whole section $D \subset \mathbb{C}$. We choose a sequence of grid points $z_i \in D$, $i = 1, 2, 3, \ldots$, and in each z_i determine the smallest ε for which $z_i \in \Sigma_\varepsilon(T)$ by a singular value decomposition of the matrix $zI - T$. By interpolating the obtained values, we can then decide whether a point $z \in \mathbb{C}$ approximately belongs to $\Sigma_\varepsilon(T)$.

4.1. Computation of eigenvalues

For computing the eigenvalues of a matrix $T \in \mathbb{R}^{n\times n}$ of moderate size, one usually uses the QR-method. However, the work count of this algorithm growths very rapidly with the dimension of the matrix such that one may apply it only to an appropriately pre-processed matrix with the same eigenvalues. By a sequence of reduction steps the *Arnoldi algorithm* leads to a lower-dimensional upper Hessenberg matrix the eigenvalues of which approximate those of T:

$$H_k = \begin{pmatrix} h_{1,1} & h_{1,2} & h_{1,3} & \cdots & h_{1,m} \\ h_{2,1} & h_{2,2} & h_{2,3} & \cdots & h_{2,m} \\ 0 & h_{3,2} & h_{3,3} & \cdots & h_{3,m} \\ \vdots & \ddots & \ddots & \ddots & \vdots \\ 0 & \cdots & 0 & h_{m,m-1} & h_{m,m} \end{pmatrix}.$$

For the computation of the eigenvalues of such a matrix the QR algorithm is very efficient.

The Arnoldi method constructs a *Krylov space* $K_m = \mathrm{span}\{q, Tq, .., T^{m-1}q\}$ of dimension $m \ll n$ for an arbitrarily chosen starting vector $q \in \mathbb{R}^n$. Then, an l_2-orthonormal basis $\{v_i\}_{i=1}^m$ is computed. For this the basic algorithm is the classical Gram-Schmidt method, stabilized variants of this or, for larger m, the Householder algorithm (see Saad [29]). To the orthonormal Krylov basis $\{v_1, ..., v_m\}$, we associate the matrix $V_m := [v_1, ..., v_m] \in \mathbb{R}^{n\times m}$. Then the Hessenberg matrix $H_m \in \mathbb{R}^{m\times m}$ satisfies $H_m := V_m^T T V_m$. For this reduced matrix the QR-algorithm only requires $\mathcal{O}(m^2)$ operations in contrast to the $\mathcal{O}(n^3)$ operations, which would be required for the full matrix T. The Krylov space contains approximations mainly to the eigenvectors corresponding to those eigenvalues of T with largest modulus, which in turn are related to the desired eigenvalues of the differential operator with smallest real parts. Enlarging the dimension m of K_m improves the accuracy of this approximation as well as the number of the approximated "largest" eigenvalues. In fact, the pseudospectrum of H_m converges to that of T for $m \to n$.

The construction of the Krylov space K_m is the most cost-intensive part of the whole algorithm. It requires m-times the application of the matrix T, which amounts to the consecutive solution of the m linear systems

$$\begin{bmatrix} S & B \\ B^T & 0 \end{bmatrix} \begin{bmatrix} \tilde{v}_j \\ q_j \end{bmatrix} = \begin{bmatrix} M & 0 \\ 0 & 0 \end{bmatrix} \begin{bmatrix} v_{j-1} \\ 0 \end{bmatrix}, \quad v_j := \|\tilde{v}_j\|^{-1}\tilde{v}_j, \quad j = 2, \ldots, m. \quad (66)$$

This is achieved by a (geometric) multigrid method implemented in the software package GASCOIGNE (see [9]). Since GASCOIGNE does not support complex arithmetic the system (66) needs to be rewritten in real arithmetic, e.g.,

$$Sx = y \quad \Leftrightarrow \quad \begin{pmatrix} \mathrm{Re}S & \mathrm{Im}S \\ -\mathrm{Im}S & \mathrm{Re}S \end{pmatrix} \begin{pmatrix} \mathrm{Re}x \\ -\mathrm{Im}x \end{pmatrix} = \begin{pmatrix} \mathrm{Re}y \\ -\mathrm{Im}y \end{pmatrix}.$$

For the reliable approximation of the pseudospectrum of T in the subregion $D \subset \mathbb{C}$ it is necessary to choose the dimension m of the Krylov space sufficiently

large, such that all eigenvalues of T and of its perturbations in D are well approximated by eigenvalues of H_m. Further, the QR-method is to be used with maximum accuracy requiring the corresponding error tolerance TOL_2 to be set in the range of the machine accuracy. An eigenvector e_λ corresponding to an eigenvalue $\lambda \in \Sigma(H_m)$ is then obtained by solving the singular system

$$(H_m - \lambda I)e_\lambda = 0. \tag{67}$$

By back-transformation of this eigenvector from the Krylov space K_m into the ansatz space V_m, we obtain a corresponding approximate eigenvector of the full matrix T.

4.2. Computation of the pseudospectrum

Actually, we want to determine the ε-pseudospectrum of the discrete operator $\mathcal{A}_h$, which approximates the unbounded differential operator $\mathcal{A}$. The inverse Hessenberg matrix H_m^{-1} may be viewed as a low-dimensional approximation to $\mathcal{A}_h$. Consequently, we compute the ε-pseudospectrum of H_m^{-1} as approximation to that of $\mathcal{A}_h$ and eventually to that of $\mathcal{A}$. To this end, we choose a section $D \subset \mathbb{C}$, in which we want to determine the pseudospectrum. Let $D := \{z \in \mathbb{C} |\ \{\mathrm{Re}z, \mathrm{Im}z\} \in [a_r, b_r] \times [a_i, b_i]\}$ for certain values $a_r < b_r$ and $a_i < b_i$. For each $z \in D \backslash \Sigma(H_m^{-1})$ the quantity $\varepsilon(z, H_m^{-1}) := \|(zI - H_m^{-1})^{-1}\|^{-1}$ determines the smallest $\varepsilon > 0$, such that $z \in \Sigma_\varepsilon(H_m^{-1})$. The most effective way for computing the pseudospectrum goes via its definition using the smallest singular value, i.e.,

$$\varepsilon(z, H_m^{-1}) = \Sigma_{\min}(zI - H_m^{-1}). \tag{68}$$

Then, for any point $z \in D$, by computing $\Sigma_{\min}(zI - H_m^{-1})$, we obtain an approximation of the smallest ε, such that $z \in \Sigma_\varepsilon(H_m^{-1})$.

To determine the pseudospectrum in the complete rectangle D, we cover D by a grid with spacing d_r and d_i, such that k points lie on each grid line. For each grid point, we compute the corresponding ε-pseudospectrum. This requires the frequent computation of the singular value decomposition of a Hessenberg matrix. For that, we use the LAPACK routine *dgesvd* within MATLAB. Since the work count of the singular value decomposition growth like $\mathcal{O}(m^2)$, we limit the dimension of the Krylov space by $m \leq 200$.

4.2.1. Choice of parameters and accuracy issues

The described algorithm for computing the pseudospectrum of a differential operator at various stages requires the appropriate choice of parameters:

- The mesh size h in the finite element discretization on the domain $\Omega \subset \mathbb{R}^n$ for reducing the infinite dimensional problem to an matrix eigenvalue problem of dimension n_h.

- The dimension of the Krylov space $K_{m,h}$ in the Arnoldi method for the reduction of the n_h-dimensional matrix T_h to the much smaller Hessenberg matrix $H_{m,h}$.

- The size of the subregion $D := [a_r, b_r] \times [a_i, b_i] \subset \mathbb{C}$ in which the pseudospectrum is to be determined and the mesh width k of interpolation points in $D \subset \mathbb{C}$.

Only for an appropriate choice of these parameters one obtains a reasonable approximation to the pseudospectrum of the differential operator $\mathcal{A}$. First, h is refined and m is increased until no significant change in the boundaries of the ε-pseudospectrum is observed anymore. Decreasing k yields an improved resolution of the ε-pseudospectrum's boundary. But there is not much accuracy gained beyond a resolution of 100×100 image points in the rectangle D.

4.3. Numerical test

As a prototypical example for the proposed algorithm, we consider the Sturm-Liouville boundary value problem (see Trefethen [33])

$$\mathcal{A}u(x) = -u''(x) - q(x)u(x), \quad x \in \Omega = (-10, 10), \tag{69}$$

with the complex potential $q(x) := (3 + 3\mathbf{i})x^2 + \frac{1}{16}x^4$, and the boundary condition $u(-10) = 0 = u(10)$. Using the sesquilinear form

$$a(u, v) := (u', v') + (qu, v), \quad u, v \in H_0^1(\Omega),$$

the eigenvalue problem of the operator $\mathcal{A}$ reads in variational form

$$a(v, \varphi) = \lambda(v, \varphi) \quad \forall \varphi \in H_0^1(\Omega). \tag{70}$$

First, the interval $\Omega = (-10, 10)$ is discretized by eightfold uniform refinement resulting in the finest mesh size $h = 20 \cdot 2^{-8} \approx 0.078$ and $n = 256$. The Arnoldi algorithm for the corresponding discrete eigenvalue problem of the inverse operator $\mathcal{A}^{-1}$ generates a Hessenberg matrix of dimension $m = 200$. The resulting reduced eigenvalue problem is solved by the QR method. For the determination of the corresponding pseudospectra, we export the Hessenberg matrix H_m into a MATLAB file. For this, we use the routine *DGESVD* in *LAPACK* (singular value decomposition) on meshes with 10×10 and with 100×100 points. The ε-pseudospectra are computed for $\varepsilon = 10^{-1}, 10^{-2}, ..., 10^{-10}$ leading to the results shown in Figure 2.

We observe that all eigenvalues have negative real part but also that the corresponding pseudospectra reach far into the positive half-plane of $\mathbb{C}$, i.e., small perturbations of the matrix may have strong effects on the location of the eigenvalues. Further, we see that already a grid with 10×10 points yields sufficiently good approximations of the pseudospectrum of the matrix H_m (resp. the considered differential operator). The costly refinement to 100×100 points only smoothens out the borderlines of $\Sigma_\varepsilon(H_m)$. These results coincide with those reported in Trefethen [33], demonstrating the correctness of our code.

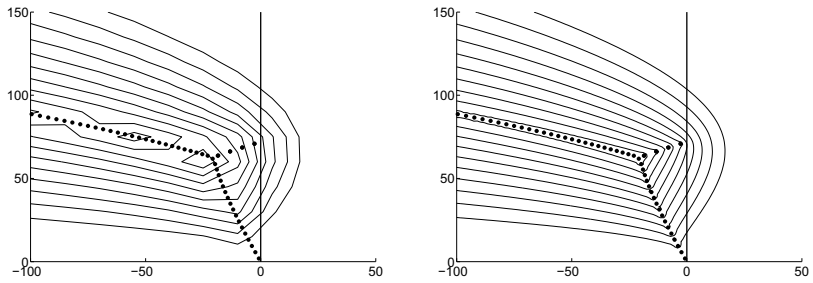

Figure 2: Approximate eigenvalues and pseudospectra of the operator $\mathcal{A}$ computed from those of the operator $\mathcal{A}^{-1}$ on a 10×10 grid (left) and on a 100×100 grid (right): dots represent eigenvalues and the lines the boundaries of the ε-pseudospectra for $\varepsilon = 10^{-1}, ..., 10^{-10}$.

5. The Burgers equation

5.1. Formulation of the stability problem

The first PDE test example is the two-dimensional *Burgers equation*

$$-\nu\Delta v + v \cdot \nabla v = 0, \quad \text{in } \Omega. \tag{71}$$

This equation is sometimes considered as a simplified version of the "incompressible" Navier-Stokes equation since both equations contain the same nonlinearity. Here, we investigate the stability properties of the Burgers operator by taking into account different choices of possible "inflow" boundary conditions, Dirchlet or Neumann, which amounts to different types of admissible perturbations in the stability analysis. Further, we also use this example for investigating some questions related to the numerical techniques used, e.g., the required dimension of the Krylov spaces in the Arnoldi method.

For simplicity, we choose $\Omega := (0,2) \times (0,1) \subset \mathbb{R}^2$, and along the left-hand "inflow boundary" $\Gamma_{\text{in}} := \partial\Omega \cap \{x_1 = 0\}$ as well as along the upper and lower boundary parts $\Gamma_{\text{rigid}} := \partial\Omega \cap (\{x_2 = 0\} \cup \{x_2 = 1\})$ Dirichlet conditions and along the right-hand "outflow boundary" $\Gamma_{\text{out}} := \partial\Omega \cap \{x_1 = 2\}$ Neumann conditions are imposed, such that the exact solution has the form $\hat{v}(x) = (x_2, 0)$ of a Couette-like flow. We set $\Gamma_D := \Gamma_{\text{rigid}} \cup \Gamma_{\text{in}}$ and choose $\nu = 10^{-2}$. Linearization around this stationary solution yields the nonsymmetric stability eigenvalue problem for $v = (v_1, v_2)$:

$$\begin{aligned} -\nu\Delta v_1 + x_2\partial_1 v_1 + v_2 &= \lambda v_1, \\ -\nu\Delta v_2 + x_2\partial_1 v_2 &= \lambda v_2, \end{aligned} \tag{72}$$

in Ω with the boundary conditions $v|_{\Gamma_D} = 0$, $\partial_n v|_{\Gamma_{\text{out}}} = 0$. For discretizing this problem, we use the finite element method described above with conforming Q_1-elements combined with transport stabilization by the SUPG (streamline upwind Petrov-Galerkin) method of Hughes & Brooks [17].

5.2. Computation of pseudospectra

We investigate the eigenvalues of the linearized (around Couette flow) Burgers operator with Dirichlet or Neumann inflow conditions. We use the Arnoldi method described above with Krylov spaces of dimension $m = 100$ or $m = 200$. For generating the contour lines of the ε-pseudospectra, we use a grid of 100×100.

For testing the accuracy of the proposed method, we compare the quality of the pseudospectra computed on meshes of width $h = 2^{-7}$ and $h = 2^{-8}$ and using Krylov spaces of dimension $m = 100$ or $m = 200$. The results shown in Figure 3 and Figure 4 indicate that the choice $h = 2^{-7}$ and $m = 100$ is sufficient for the present example.

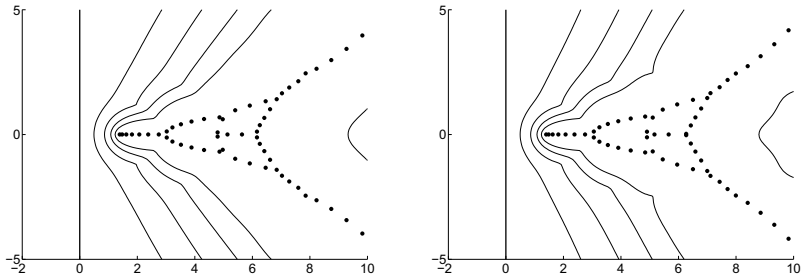

Figure 3: Computed pseudospectra of the linearized Burgers operator with **Dirichlet** inflow condition for $\nu = 0.01$ and $h = 2^{-7}$ (left) and $h = 2^{-8}$ (right) computed by the Arnoldi method with $m = 100$. The dots represent eigenvalues and the lines the boundaries of the ε-pseudospectra for $\varepsilon = 10^{-1}, ..., 10^{-4}$.

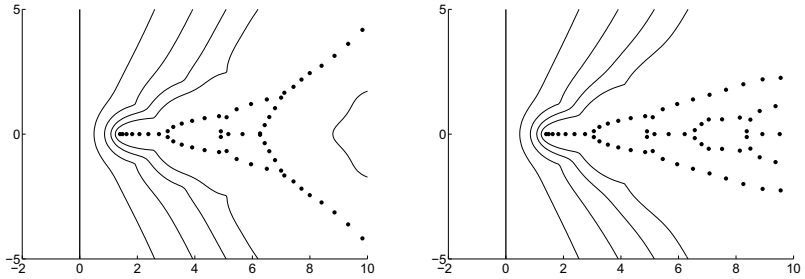

Figure 4: Computed pseudospectra of the linearized Burgers operator with **Dirichlet** inflow condition for $\nu = 0.01$ and $h = 2^{-8}$ computed by the Arnoldi method with $m = 100$ (left) and $m = 200$ (right). The dots represent eigenvalues and the lines the boundaries of the ε-pseudospectra for $\varepsilon = 10^{-1}, ..., 10^{-4}$.

Now, we turn to Neumann inflow conditions. In this particular case the first eigenvalues and eigenfunctions of the linearized Burgers operator can be determined analytically as $\lambda_k = \nu k^2 \pi^2$, $v_k(x) = (\sin(k\pi x_2), 0)^T$, for $k \in \mathbb{Z}$. All these eigenvalues are degenerate. However, there exists another eigenvalue

$\lambda_4 \approx 1.4039$ between the third and fourth one, which is not of this form, but also degenerates.

We use this situation for studying the dependence of the proposed method for computing pseudospectra on the size of the viscosity, $0.001 \leq \nu \leq 0.01$. Again the discretization uses the mesh size $h = 2^{-7}$, Krylov spaces of dimension $m = 100$ and a grid of spacing $k = 100$. By varying these parameters, we find that only eigenvalues with $\mathrm{Re}\lambda \leq 6$ and corresponding ε-pseudospectra with $\varepsilon \geq 10^{-4}$ are reliably computed. The results are shown in Figure 5.

For Neumann inflow conditions the most critical eigenvalue is significantly smaller than the corresponding most critical eigenvalue for Dirichlet inflow conditions, which suggests weaker stability properties in the "Neumann case". Indeed, in Figure 5, we see that the 0.1-pseudospektrum reaches into the negative complex half-plane indicating instability for such perturbations. This effect is even more pronounced for $\nu = 0.001$ with $\lambda^N_{\mathrm{crit}} \approx 0.0098$.

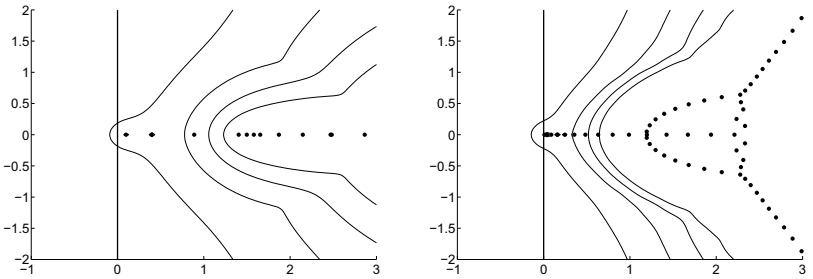

Figure 5: Computed pseudospectra of the linearized (around Couette flow) Burger operator with **Neumann** inflow conditions for $\nu = 0.01$ (left) and $\nu = 0.001$ (right): The dots represent eigenvalues and the lines the boundaries of the ε-pseudospectra for $\varepsilon = 10^{-1}, \ldots, 10^{-4}$.

6. The Navier-Stokes equations

In this section, we investigate the stability of some stationary solutions of the Navier-Stokes equations. These are the classical Couette and Poiseuille flows and the flow in the benchmark problem "channel flow around a cylinder" (see Schäfer & Turek [30].

6.1. Couette flow

At first, we consider 2D shear flow (so-called Couette flow), i.e., the flow between two infinite plates which are moved parallel to each other with constant relative velocity $\hat{v}_1 \equiv 1$. We choose the same reference domain $\Omega = (0, 2) \times (0, 1)$ as considered above for the Burgers equation. Then, neglecting gravity Couette flow is given by $\hat{v}(x) = (x_2, 0)^T$ with $\hat{p}(x) \equiv 0$, which is divergence free and satisfies the equation for all Reynolds numbers. Couette flow satisfies the Dirichlet boundary conditions $\hat{v}|_{x_2=0} = 0$, $\hat{v}|_{x_2=1} = 1$ and several different

possible inflow and outflow boundary conditions. Here, as in the preceding section, we consider the following two options:

$$\text{Dirichlet inflow:} \quad \hat{v}|_{\Gamma_{\text{in}}} = x_2, \quad \nu\partial_n\hat{v} - \hat{p}n|_{\Gamma_{\text{out}}=0}, \tag{73}$$

$$\text{Neumann inflow:} \quad \nu\partial_n\hat{v} - \hat{p}n|_{\Gamma_{\text{in}}} = 0, \quad \nu\partial_n\hat{v} - \hat{p}n|_{\Gamma_{\text{out}}} = 0. \tag{74}$$

Remark 6.1. As a third alternative, we may consider perturbations satisfying periodic boundary conditions $\hat{v}|_{\Gamma_{\text{in}}} = \hat{v}|_{\Gamma_{\text{out}}}$. However, in our test calculations the results obtained for periodic boundary conditions largely coincide with those for Neumann/Neumann boundary conditions (74), so that we do not further discuss this special case.

After linearization of the Navier-Stokes operator around Couette flow, we obtain the following eigenvalue problem

$$\begin{aligned} -\nu\Delta v_1 + x_2\partial_1 v_1 + \partial_1 p + v_2 &= \lambda v_1, \\ -\nu\Delta v_2 + x_2\partial_1 v_2 + \partial_2 p &= \lambda v_2, \\ \partial_1 v_1 + \partial_2 v_2 &= 0. \end{aligned} \tag{75}$$

The discretization is done by the finite element method using GLS stabilization as described above for the general Navier-Stokes problem.

Remark 6.2. For moderate Reynolds numbers similar results coinciding by three decimals on the finest mesh are obtained by LPS stabilization and by the inf-sup stable Taylor-Hood element. This shows that pressure stabilization does not much affect the accuracy in computing eigenvalues. However, this is completely different in the case of higher Reynolds numbers when transport stabilization is required. Here, the kind of stabilization may drastically affect the accuracy in computing eigenvalues, as we will see below.

6.1.1. Eigenvalues and eigenvectors

The only difference between the eigenvalue problem (75) for the Navier-Stokes equation and (72) for the Burgers equation is the additional incompressibility constraint and the presence of the pressure variable. This implies that in the case of Neumann inflow conditions the explicitly given eigenvalues and divergence-free eigenfunctions, $\lambda_k = k^2\pi^2$, $v_k = (\sin(k\pi x_2), 0)^T$, $k \in \mathbb{Z}$, are also eigenfunctions of (75) corresponding to the pressure component $p \equiv 0$. Since the associated generalized eigenvectors $w_k = (\sin(k\pi x_2), \sin(k\pi x_2))^T$ of the Burgers equation are not divergence free, these eigenvalues of (75) are non-degenerate in contrast to the eigenvalues of the burgers equation (72). The eigenvalues and corresponding pseudospectra are again computed on meshes with $h = 2^{-7}$ and using Krylov spaces of dimension $m = 200$. The obtained eigenvalues are listed in Table 1. These eigenvalues are simple in contrast to the same situation in the context of the Burgers operator. In addition to the explicitly given eigenvalues $\lambda_k = k^2\pi^2$ there are further ones, corresponding to eigenmodes with nonzero pressure. These "new" eigenvalues are not eigenvalues of the Burgers operator.

Table 1: Computed first six eigenvalues, numbered in consecutive order, of the linearized (around Couette flow) Navier-Stokes operator with **Neumann** inflow conditions for $\nu = 0.01$.

h	1	3	5	6	h	2	4
2^{-5}	0.09878	0.3961	0.8947	1.600	2^{-5}	0.2389	0.8802
2^{-6}	0.09872	0.3951	0.8899	1.584	2^{-6}	0.2390	0.8746
2^{-7}	0.09870	0.3949	0.8887	1.580	2^{-7}	0.2392	0.8737
$\lambda = \nu k^2 \pi^2$	0.09870	0.3948	0.8883	1.579	ref.	0.2395	0.8743

6.1.2. Pseudospectra

Next, we investigate the pseudospectra of the linearized Navier-Stokes operator compared to those of the linearized Burgers operator. The results are shown in Figures 6 and 7. The accuracy of the obtained pseudospectra is confirmed by test computations on finer meshes with $h = 2^{-8}$ using larger Krylov spaces with dimension $m = 200$ and different stabilization parameters in the finite element discretization. It turns out that in both cases the stability properties are similar. But for the Burgers operator only the 10^{-1}-pseudospectrum reaches into the negative complex half-plane, while for the Navier-Stokes operator the 10^{-2}-pseudospectrum touches the imaginary axes.

6.1.3. Pseudospectra for larger Reynolds numbers

In Trefethen et al. [36] it is stated that in experiments Couette flow turns nonstationary for a Reynolds number $\mathrm{Re}_{\mathrm{crit}}$ in the interval $350 \leq \mathrm{Re}_{\mathrm{crit}} \leq 3500$, where in the present situation $\mathrm{Re} = \nu^{-1}$. The computed pseudospectrum for $\mathrm{Re} = 350$ and $\mathrm{Re} = 3500$ with Neumann inflow conditions are shown in Figure 8. Again the correctness of these results is confirmed by testing on finer meshes with larger Krylov spaces and different stabilization parameters. Our results differ somewhat from those in Trefethen et al. [36] as our ε-pseudospectra reach further into the negative complex half-plane.

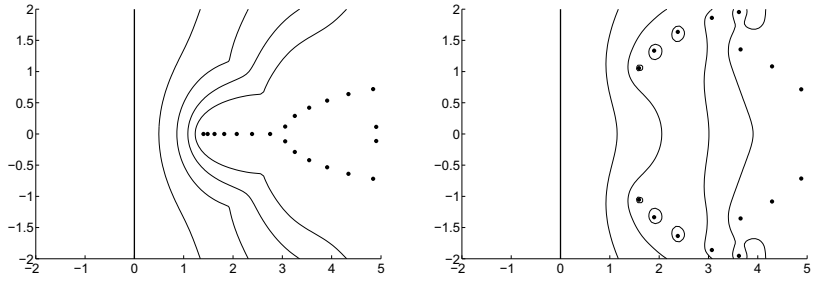

Figure 6: Computed pseudospectra of the linearized (around Couette flow) Burgers (left) and Navier-Stokes operator (right) for $\nu = 0.01$ and **Dirichlet** inflow condition: The dots represent eigenvalues and the lines the boundaries of the ε-pseudospectra for $\varepsilon = 10^{-1}, \ldots, 10^{-4}$.

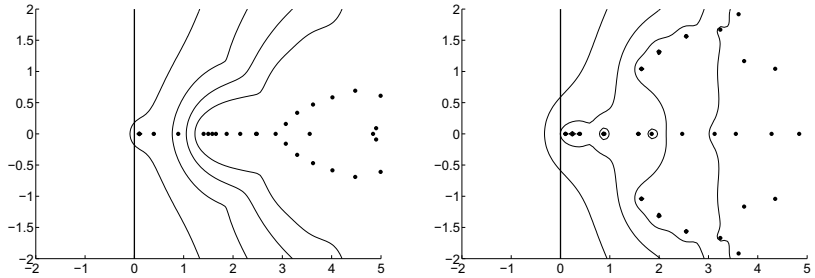

Figure 7: Computed pseudospectra of the linearized (around Couette flow) Burgers (left) and Navier-Stokes operator (right) with **Neumann** inflow conditions for $\nu = 0.01$: The dots represent eigenvalues and the lines the boundaries of the ε-pseudospectra for $\varepsilon = 10^{-1}, \ldots, 10^{-4}$.

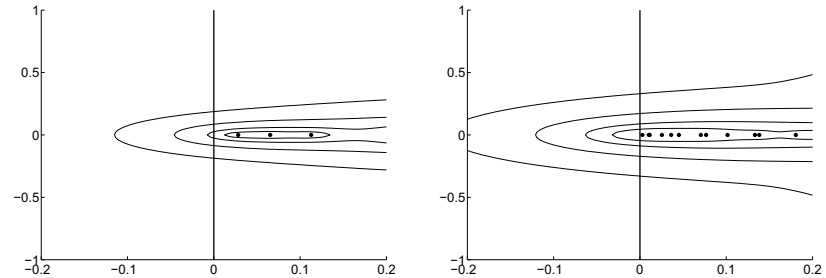

Figure 8: Computed pseudospectra of the linearized (around Couette flow) Navier-Stokes operator with **Neumann** inflow conditions for Re = 350 (left) and Re = 3500 (right) using GLS stabilization: The dots represent eigenvalues and the lines the boundaries of the ε-pseudospectra for $\varepsilon = 10^{-2}, 10^{-2.5}, 10^{-3}, 10^{-3.5}$.

6.1.4. Effect of stabilization

Before we conclude this section we need to give a comment concerning the effects of using different kinds of transport stabilization in the finite element discretization.

As depicted in Table 2 the computed smallest eigenvalue depends strongly on the choice of the stabilization. More into details, we see, that the pressure stabilization has little influence, hence the results using equal order Q_1 elements give approximately the same values as the inf-sup stable Taylor-Hood element. However, the choice of the transport stabilization strongly influences the computed discrete eigenvalue, although under sufficient refinement the difference will vanish. We immediately see in Figure 9 that this also influences our computed pseudospectra. Nonetheless, these computations are not worthless, since the different computed eigenvalues using different transport stabilizations immediately show that a critical pseudospectrum for perturbations of the size of the stabilization exists.

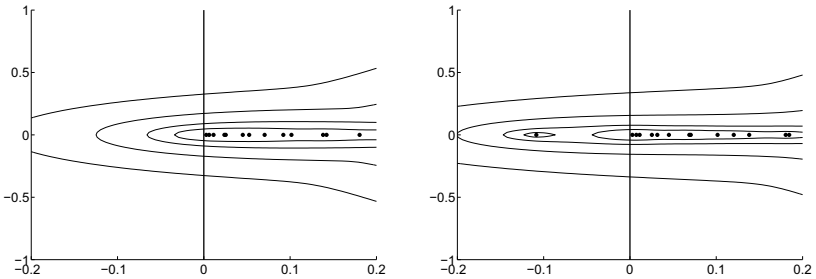

Figure 9: Computed pseudospectra of the linearized (around Couette flow) Navier-Stokes operator with **Neumann** inflow conditions for $\mathrm{Re} = 3500$ using the inf-sup stable Taylor-Hood element with GLS (left) and LPS (right) transport stabilization: The dots represent eigenvalues and the lines the boundaries of the ε-pseudospectra for $\varepsilon = 10^{-2}, 10^{-2.5}, 10^{-3}, 10^{-3.5}$.

Table 2: Computed smallest eigenvalue of the linearized (around Couette flow) Navier-Stokes operator with **Neumann** inflow conditions for $\mathrm{Re} = 3500$ for different kinds of stabilization.

h	GLS (Q_1)	GLS (Taylor-Hood)	LPS (Q_1)	LPS (Taylor-Hood)
2^{-5}	0.002822	0.002820	-0.03182	0.002820
2^{-6}	0.002820	0.002820	-0.08455	-0.06330
2^{-7}	0.002820	0.002820	-0.16434	-0.14280
2^{-8}	0.002820	0.002820	-0.06297	-0.10850

6.1.5. The "deficiency test"

We use the present situation for testing the relevance of the "deficiency test" stated in Theorem 2.1 an Section 2.3.1. For this, we follow the procedure discussed in Section 2.3.1, i.e., we choose $\varepsilon = 2\mathrm{Re}\lambda_{\mathrm{crit}}\|v^*\|^{-1} \ll 1$ and check whether with the computed pseudospectrum of $\mathcal{A}'(\hat{v})$, there holds

$$\lambda_\varepsilon := \lambda_{\mathrm{crit}} - \varepsilon\|v^*\| = -\overline{\lambda}_{\mathrm{crit}} \in \Sigma_\varepsilon(\mathcal{A}'(\hat{v})). \tag{76}$$

Table 3 shows the critical eigenvalue λ_{crit} and the "test quantity" $\|v_h^*\|$ depending on the Reynolds number.

We begin with the case $\mathrm{Re} = 350$ and the critical eigenvalue $\lambda_{\mathrm{crit}}^{(350)} \approx 0.0282$. For the values $\|v^*\| \approx 450$ and $\varepsilon = 2\mathrm{Re}\lambda_{\mathrm{crit}}\|v^*\|^{-1} \approx 1.3 \cdot 10^{-4}$, there holds $\lambda_\varepsilon^{(350)} \approx -0.0282$. Next, we consider the case $\mathrm{Re} = 3500$ and the critical eigenvalue $\lambda_{\mathrm{crit}}^{(3500)} \approx 0.00282$. For the values $\|v^*\| \approx 11111$ and $\varepsilon = 2\mathrm{Re}\lambda_{\mathrm{crit}}\|v^*\|^{-1} \approx 5 \cdot 10^{-7}$, there holds $\lambda_\varepsilon^{(3500)} \approx -0.00282$. These results are in qualitative agreement with the computed ε-pseudospectra of the linearized Navier-Stokes operator shown in Figure 8, i.e., $\lambda_\varepsilon^{(350)} \in \Sigma_{10^{-3}}(\mathcal{A})$ and $\lambda_\varepsilon^{(3500)} \in \Sigma_{10^{-3.5}}(\mathcal{A})$.

Table 3: Development of the "test quantity" $\|v_h^*\|$ under mesh refinement for the critical eigenvalues of the linearized (around Couette flow) Navier-Stokes operator with **Neumann** inflow conditions for different Reynolds numbers $\mathrm{Re} = 100, \ldots, 10000$.

$h \setminus \mathrm{Re}$	100	**350**	500	1000	**3500**	5000	10000
2^{-6}	46	370	625	1290	2500	2500	2049
2^{-7}	48	416	714	1923	5882	7142	8620
2^{-8}	48	434	769	2222	11111	14285	21276
λ_{crit}	0.0987	**0.0282**	0.0197	0.00987	**0.00282**	0.00197	0.00099

6.2. Poiseuille flow

Next, we investigate the stability of Poiseuille flow. On a short channel $\Omega = (0,2) \times (0,1)$, we consider the classical Poiseuille flow,

$$\hat{v}(x) = (1 - 4(x_2 - 0.5)^2, 0)^T, \quad \hat{p}(x) = -8\nu^{-1}x_1,$$

which satisfies no-slip conditions along the upper and lower boundary and the Dirichlet inflow condition $\hat{v}(0,x_2) = (1-4(x_2-0.5)^2,0)^T$, or alternatively the Neumann inflow condition $(\nu\partial_n\hat{v} - \hat{p}n)(0,x_2) = 0$. The outflow condition is chosen of Neumann-type $(\nu\partial_n\hat{v} - \hat{p}n)(2,x_2) = 0$. Linearizing the Navier-Stokes operator around this solution yields the eigenvalue problem

$$\begin{aligned} -\nu\Delta v_1 + 4(x_2 - x_2^2)\partial_1 v_1 + \partial_1 p + 4(1-2x_2)v_2 &= \lambda v_1, \\ -\nu\Delta v_2 + 4(x_2 - x_2^2)\partial_1 v_2 + \partial_2 p &= \lambda v_2, \\ \partial_1 v_1 + \partial_2 v_2 &= 0. \end{aligned} \tag{77}$$

We only consider perturbations which are not required to satisfy any inflow or outflow conditions as this is the case which leads to smaller eigenvalues.

The most critical eigenvalues for different Reynolds numbers are shown in Table 4. Again comparing the results coming from different stabilization schemes, we conclude, that only the results for $\mathrm{Re} = 1000$ can be trusted. For larger Reynolds numbers, we see a significant difference between LPS and GLS transport stabilization, which vanishes only on increasingly refined meshes. This is similar to our findings for the linearization around Couette Flow, but since for $\mathrm{Re} \geq 6000$ the eigenvalues obtained using GLS stabilization have positive (though very small) real part these values are not yet converged.

6.2.1. Pseudospectra

According to Orszag [22] Poiseuille flow turns nonstationary at $\mathrm{Re} > 5772.22$. However, in experiments this transition is observed already for much smaller Reynolds numbers. Therefore, in Trefethen et al. [36] the ε-pseudospectra are computed for $\mathrm{Re} = 1000$ and $\mathrm{Re} = 10000$ showing a critical pseudospectrum in the latter case. Here, we consider the same Reynolds numbers and try to explain the experimentally observed instability for smaller Reynolds numbers by a

Table 4: Computed eigenvalue with smallest real part of the linearized (around Poiseuille flow) Navier-Stokes operator with **Neumann** inflow conditions for different Reynolds numbers.

(a) Transport stabilization using LPS

h/Re	100	500	1000	2000	4000	6000	10000
2^{-6}	0.04936	-0.04000	-0.1054	-0.1559	-0.1365	-0.1129	-0.0709
2^{-7}	0.04935	0.00987	-0.0120	-0.0445	-0.0877	-0.1104	-0.1313
2^{-8}	0.04935	0.00987	0.0049	-0.0035	-0.0167	-0.0286	-0.0540

(b) Transport stabilization using GLS

h/Re	100	500	1000	2000	4000	6000	10000
2^{-6}	0.04936	0.00987	0.0049	0.0025	0.0012	0.00082	0.00039
2^{-7}	0.04935	0.00987	0.0049	0.0025	0.0012	0.00082	0.00022
2^{-8}	0.04935	0.00987	0.0049	0.0025	0.0012	0.00082	0.00038

quantitative analysis of the relevant pseudospectra. To this end, we choose the maximum inflow velocity $\bar{v}_{\text{in}} = 1$, the characteristic channel width $d = 1$, and set the viscosity $\nu = 0.5 \cdot 10^{-3}$ and $\nu = 0.5 \cdot 10^{-4}$ to obtain the desired Reynolds numbers. The results are shown in Figure 10. There is only little quantitative coincidence with the results reported in Trefethen et al. [36]. Our results yield more critical pseudospectra, e.g., already the $10^{-3.5}$-pseudospectrum reaches into the negative complex half-plane.

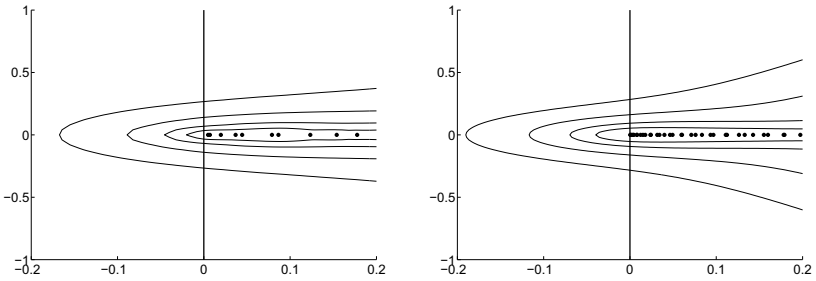

Figure 10: Computed pseudospectra of the linearized (around Poiseuille flow) Navier-Stokes operator with **Neumann** inflow conditions for Re = 1000 (left) and Re = 10000 (right) computed by the inf-sup stable Taylor-Hood element with GLS transport stabilization: The dots represent eigenvalues and the lines the boundaries of the ε-pseudospectra for $\varepsilon = 10^{-2}, 10^{-2.5}, 10^{-3}, 10^{-3.5}$.

6.2.2. The "deficiency test"

We consider the case $\text{Re} = 1000$ and the critical eigenvalue $\lambda_{\text{crit}} \approx 0.005$. For the values $\|v_h^*\| \approx 6500$ and $\varepsilon = 2\text{Re}\lambda_{\text{crit}}\|v^*\|^{-1} \approx 3 \cdot 10^{-6}$, there holds $\lambda_\varepsilon = \lambda_{\text{crit}} - \varepsilon\|v^*\| \approx -0.005$. This is in qualitative agreement with the computed

ε-pseudospectra shown in Figure 10, i.e., $\lambda_\varepsilon \in \Sigma_{10^{-3.5}}(\mathcal{A})$.

Table 5: Development of the "test quantity" $\|v_h^*\|$ under mesh refinement for the critical eigenvalues of the linearized (around Poiseuille flow) Navier-Stokes operator with **Neumann** inflow conditions for different Reynolds numbers $\mathrm{Re} = 100, 350, 500, 1000, 3500, 5000, 10000$.

Re	100	350	500	**1000**	3500	5000	10000
h	$\|v_h^*\|$						
2^{-6}	71	416	588	862	847	769	685
2^{-7}	75	625	1000	1851	3225	3448	3021
2^{-8}	76	666	1250	3030	7692	9090	10526
λ_{crit}	0.0494	0.0141	0.0099	**0.00494**	0.00141	0.00099	0.000384

6.3. The "flow channel" benchmark

The configuration of the next example is that of the (laminar) 2D flow benchmark described in Schäfer & Turek [30] (see Figure 11). The geometry data are as follows: channel domain $\Omega := (0.00\mathrm{m}, 2.2\mathrm{m}) \times (0.00\mathrm{m}, 0.41\mathrm{m})$, diameter of circle $D := 0.10\mathrm{m}$, center of circle at $a := (0.20\mathrm{m}, 0.20\mathrm{m})$ (slightly nonsymmetric position). The Reynolds number is defined in terms of the diameter D and the maximum inflow velocity $\bar{U} = \max|v^{\mathrm{in}}| = 0.3\mathrm{m/s}$ (parabolic profile), $\mathrm{Re} = \bar{U}^2 D/\nu$. The boundary conditions are

$$v|_{\Gamma_{\mathrm{rigid}}} = 0, \quad v|_{\Gamma_{\mathrm{in}}} = v^{\mathrm{in}}, \quad \nu\partial_n v - np|_{\Gamma_{\mathrm{out}}} = 0. \tag{78}$$

The viscosity is chosen such that the Reynolds number is small enough, $20 \leq \mathrm{Re} \leq 40$, to guarantee stationarity of the base flow as shown in Figure 11. For $\mathrm{Re} = 60$ the flow is nonstationary (time periodic).

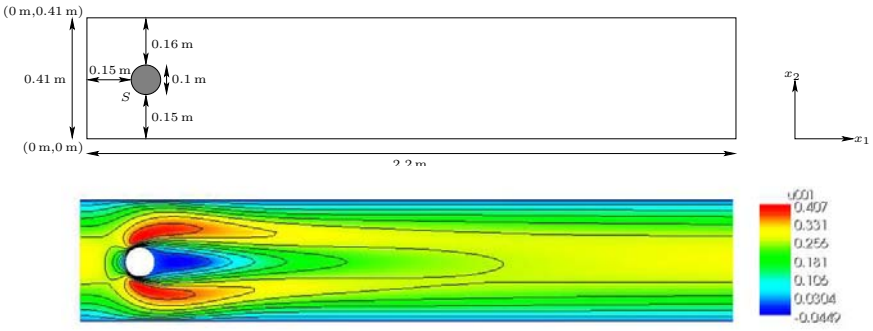

Figure 11: Configuration of the "channel flow" benchmark and x_1-component of the velocity for $\mathrm{Re} = 40$.

We want to investigate the stability of the computed base flow for several Reynolds numbers, $20 \leq \mathrm{Re} \leq 60$, and inflow conditions imposed on the admissible perturbations, Dirichlet or Neumann ("free"), by determining the corresponding critical eigenvalues and pseudospectra. This computation uses a "stationary code" employing the Newton method for linearization, which is known

to potentially yield stationary solutions even at Reynolds numbers for which such solutions may not be stable.

6.4. Perturbations satisfying Dirichlet inflow conditions

We begin with the case of perturbations satisfying (homogeneous) Dirichlet inflow conditions. Table 6 contains the computed eigenvalues for the five different Reynolds numbers $\mathrm{Re} = 20, 40, 45, 50, 60$. The eigenvalue with smallest real part at $\mathrm{Re} \gg 20$ does not correspond to that at $\mathrm{Re} = 20$. It is rather another real eigenvalue, which becomes most critical for $\mathrm{Re} \to 20$. For $\mathrm{Re} \to 60$, we have a (two-fold) eigenvalue with negative real part, which indicates instability of the computed base flow.

Next, we investigate the pseudospectra of the critical eigenvalues for $\mathrm{Re} = 40$ and $\mathrm{Re} = 60$. This is done on meshes which are obtained by four to five uniform refinements of the (locally adapted) meshes used for computing the base flow. In the Arnoldi method, we use Krylov spaces of dimension $m = 100$. Computations with $m = 200$ give almost the same results. The obtained pseudospectra are shown in Figure 12.

Table 6: Computed eigenvalue with smallest real part of the linearized ("channel flow") Navier-Stokes operator for **Dirichlet** inflow conditions and different Reynolds numbers $\mathrm{Re} = 20, 40, 45, 50, 60$.

Re	20	40	45	50	60
4	0.062	0.0200±0.33i	0.0097±0.33i	0.0011±0.33i	-0.0125±0.33i
5	0.062	0.0187±0.33i	0.0080±0.33i	-0.0010±0.34i	-0.0157±0.34i
6	0.062	0.0186±0.33i	0.0076±0.33i	-0.0016±0.34i	-0.0165±0.34i
ref.	0.062	0.0185±0.33i	0.0075±0.33i	-0.0018±0.34i	-0.0165±0.34i

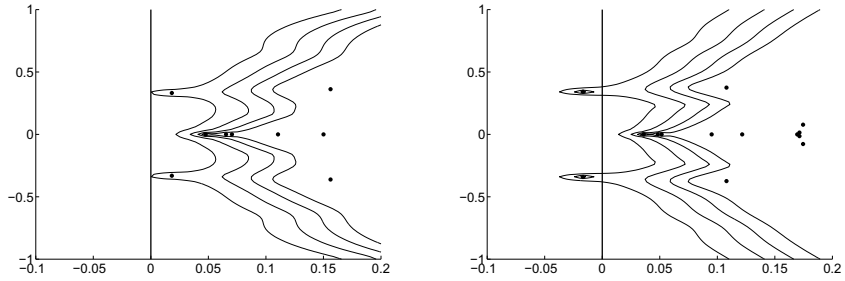

Figure 12: Computed pseudospectra of the linearized Navier-Stokes operator ("channel flow" benchmark) for different Reynolds numbers, $\mathrm{Re} = 40$ (left) and $\mathrm{Re} = 60$ (right), with **Dirichlet** inflow conditions: The dots represent eigenvalues and the lines the boundaries of ε-pseudospectra for $\varepsilon = 10^{-2}, 10^{-2.5}, 10^{-3}, 10^{-3.5}$.

For $\mathrm{Re} = 40$ the relevant 10^{-2}-pseudospectrum does not reach into the negative complex half-plane indicating stability of the corresponding base solution

in this case, as expected in view of the result of nonstationary computations. Obviously the transition from stationary to nonstationary (time periodic) solutions occurs in the range $40 \leq \mathrm{Re} \leq 60$. However, for this "instability" the sign of the real part of the critical eigenvalue seems to play the decisive role and not so much the size of the corresponding pseudospectrum. This is reflected by the results shown in Table 7, which demonstrate that the test quantity $\|v_h^*\|$ remains uniformly bounded for the range of Reynolds numbers considered.

Table 7: Development of the "test quantity" $\|v_h^*\|$ under mesh refinement for the critical eigenvalues of the linearized (around the "channel flow") Navier-Stokes operator with **Dirichlet** inflow conditions for different Reynolds numbers $\mathrm{Re} = 20, 40, 45, 50, 60$.

Re	20	40	45	50	60
level	$\|v_h^*\|$				
4	31	11	10	10	10
5	31	12	11	11	10
6	31	13	12	11	11
$\mathrm{Re}\lambda_{\mathrm{crit}}$	0.0624	0.0186	0.0076	-0.00106	-0.0165

6.4.1. Perturbations satisfying Neumann (free) inflow conditions

Now, we consider the case of perturbations satisfying (homogeneous) Neumann ("free") inflow conditions, i.e., the space of admissible perturbations is larger than in the preceding case. In view of the observations made before for Couette flow and Poiseuille flow, we expect weaker stability properties. The stationary base flow is again computed using Dirichlet inflow conditions but the associated eigenvalue problem of the linearized Navier-Stokes operator is considered with Neumann inflow conditions. Table 8 contains the results. In the case of perturbations satisfying Dirichlet inflow conditions the stationary base flow turned out to be stable up to $\mathrm{Re} = 45$. In the present case of perturbations satisfying Neumann inflow conditions at $\mathrm{Re} = 40$ the critical eigenvalue has positive but very small real part, $\mathrm{Re}\lambda_{\mathrm{min}} \approx 0.003$. Hence, the precise stability analysis requires the determination of the corresponding pseudospectrum. The results are shown in Figure 13. Though, for $\mathrm{Re} = 40$ the real part of the most critical (positive) eigenvalue is rather small, the corresponding 10^{-2}-pseudospectrum reaches only a little into the negative complex half-plane.

Table 8: Computed eigenvalues with smallest real part of the linearized ("channel flow") Navier-Stokes operator with **Neumann** inflow conditions for $\mathrm{Re} = 20, 40, 45, 50, 60$.

Re	20	40	45	50	60
4	0.0150	0.005±0.00i	0.0002±0.16i	-0.0054±0.16i	-0.0140±0.17i
5	0.0152	0.004±0.16i	-0.0043±0.16i	-0.0110±0.16i	-0.0217±0.17i
6	0.0153	0.003±0.16i	-0.0049±0.16i	-0.0119±0.16i	-0.0232±0.17i
ref.	0.0154	0.003±0.16i	-0.0052±0.16i	-0.0120±0.16i	-0.0240±0.17i

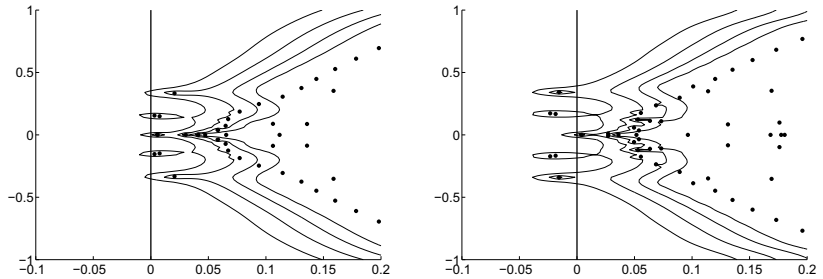

Figure 13: Computed pseudospectra of the linearized Navier-Stokes operator ("channel flow") with **Neumann** inflow conditions for different Reynolds numbers, $\mathrm{Re} = 40$ (left) and $\mathrm{Re} = 60$ (right): The dots represent eigenvalues and the lines the boundaries of the ε-pseudospectra for $\varepsilon = 10^{-2}, 10^{-2.5}, 10^{-3}, 10^{-3.5}$.

Table 9: Development of the "test quantity" $\|v_h^*\|$ under mesh refinement for the critical eigenvalues of the linearized (around the "channel flow") Navier-Stokes operator with **Neumann** inflow conditions for different Reynolds numbers $\mathrm{Re} = 20, 40, 45, 50, 60$.

Re	20	40	45	50	60
level	$\|v_h^*\|$				
4	15	30	27	29	32
5	15	25	27	27	30
6	15	24	25	25	28
$\mathrm{Re}\lambda_{\mathrm{crit}}$	0.015	0.003	-0.005	-0.012	-0.024

7. Conclusion

The results presented above lead us to the following conclusions concerning the guiding questions posed in the introduction:

1. In case of "laminar" Reynold numbers the computed pseudospectra turn out to be reliable for moderately fine meshes with $h \approx 2^{-7} - 2^{-8}$ and dimensions $m = 100 - 200$ of Krylov spaces.
2. The computed pseudospectra are not very sensitive with respect to the stabilization of pressure used in the finite element discretization. However, there is strong sensitivity with respect to stabilization of transport. Here, GLS gives reasonable results on coarser meshes while LPS requires rather fine meshes in order to avoid the occurrence of spurious eigenvalues.
3. The critical pseudospectrum of the linearized Navier-Stokes operator is approximated by that its of discretized analogue with optimal order.
4. The "deficiency test" $\limsup_{h\to 0} \|v_h^*\| \gg 1$ proposed in Section 2.3.1 can be used for predicting the presence of a critical pseudospectrum.
5. Generally, the base flows considered are much less stable with respect to perturbations satisfying Neumann ("free") inflow conditions than Dirichlet inflow conditions.
6. The linearized Burgers operator has significantly different stability properties than the linearized Navier-Stokes operator.

References

[1] R. Becker and M. Braack: *A two-level stabilization scheme for the Navier-Stokes equations*, Numerical Mathematics and Advanced Applications, Proc. ENUMATH 2003 (M. Feistauer et al., eds), pp. 123–130, Springer, Heidelberg, 2004.

[2] J. H. Bramble and J. E. Osborn: *Rate of convergence estimates for nonselfadjoint eigenvalue approximations*, Math. Comp. 27, 525–545 (1973).

[3] H. Chen: *Pointwise error estimates for finite element solutions of the Stokes problem*, SIAM J. Numer. Anal. 44, 1–28 (2006).

[4] P. G. Ciarlet: *Finite Element Methods for Elliptic Problems*, North-Holland, Amsterdam, 1978.

[5] N. Dunford and J. T. Schwartz: *Linear Opertaors, Part 1: General Theory*, Interscience Publishers, New York, 1957.

[6] R. G. Duran and R. H. Nochetto: *Pointwise accuracy of a stable Petrov-Galerkin approximation to the Stokes problem*, SIAM J. Numer. Anal. 6, 1395–1406 (1989).

[7] L. P. Franca, S. L. Frey, and T. J. R. Hughes: *Stabilized finite element methods: II. The incompressible Navier-Stokes equations*, Comput. Meth. Appl. Mech. Engrg. 99, 209–233 (1992).

[8] G. P. Galdi: *An Introduction to the Mathematical Theory of the Navier-Stokes Equations. Vol. 1: Linearized Steady problems, Vol. 2: Nonlinear Steady Problems*, Springer: Berlin-Heidelberg-New York, 1998.

[9] Gascoigne: *High Performance Adaptive Finite Element Toolkit*, URL: http://gascoigne.uni-hd.de, University of Heidelberg.

[10] D. Gerecht: *Pseudospektren in der Hydrodynamische Stabilitätstheorie*, Diploma thesis, Institute of Applied Mathematics, University of Heidelberg, 2010.

[11] V. Girault, R. H. Nochetto, and R. Scott: *Maximum-norm stability of the finite element Stokes projection*, J. Math. Pures Appl. 84, 279–330 (2005).

[12] V. Girault and P. A. Raviart: *Finite Element Methods for Navier-Stokes Equations*, Springer, Berlin-Heidelberg, 1986.

[13] V. Heuveline and C. Bertsch: *On multigrid methods for the eigenvalue computation of non-selfadjoint elliptic operators*, East-West J. Numer. Math. 8, 275–297 (2000).

[14] V. Heuveline and R. Rannacher: *A posteriori error control for finite element approximations of elliptic eigenvalue problems*, Advances in Comput. Math. 15, 1–32 (2001).

[15] V. Heuveline and R. Rannacher: *Adaptive FE eigenvalue approximation with application to hydrodynamic stability analysis*, Proc. Int. Conf. Advances in Numerical Mathematics, Moscow, Sept. 16-17, 2005 (W. Fitzgibbon et al., eds), pp. 109–140, Institute of Numerical Mathematics RAS, Moscow, 2006.

[16] J. Heywood, R. Rannacher, and S. Turek: *Artificial boundaries and flux and pressure conditions for the incompressible Navier-Stokes equations*, Int. J. Comput. Fluid Mech. 22, 325-352 (1996).

[17] T. J. R. Hughes and A. N. Brooks: *Streamline upwind/Petrov Galerkin formulations for convection dominated flows with particular emphasis on the incompressible Navier-Stokes equation*, Comp. Math. Appl. Mech. Engrg. 32, 199–259 (1982).

[18] T. J. R. Hughes, L. P. Franca, and M. Balestra: *A new finite element formulation for computational fluid dynamics: V. Circumvent the Babuska-Brezzi condition: A stable Petrov-Galerkin formulation for the Stokes problem accomodating equal order interpolation*, Comp. Meth. Appl. Mech. Engrg. 59, 89–99 (1986).

[19] C. Johnson, R. Rannacher and M. Boman: *Numerics and hydrodynamic stability: Towards error control in CFD*, SIAM J. Numer. Anal. 32, 1058–1079 (1995).

[20] T. Kato: *Perturbation Theory for Linear Operators*, Springer, Berlin-Heidelberg-New York, 1966.

[21] H. O. Kreiss: *Über die Stabilitätsdefinition für Differenzengleichungen, die partielle Differentialgleichungen approximieren*, Nordisk Tidskr. Informations-Behandling 2, 153–181 (1962).

[22] S. Orszag: *Accurate solution of the Orr-Sommerfeld stability equation*, J. Fluid Mech. 50, 689–703 (1971).

[23] J. E. Osborn: *Spectral approximation for compact operators*, Math. Comp. 29, 712–725 (1975).

[24] A. Quarteroni and A. Valli: *Numerical Approximation of Partial Differential Equations*, Springer, Berlin-Heidelberg-New York, 1991.

[25] R. Rannacher: *Finite element methods for the incompressible Navier-Stokes equations*, Fundamental Directions in Mathematical Fluid Mechanics (G. P. Galdi, J. Heywood, R. Rannacher, eds), pp. 191–293, Birkhäuser, Basel-Boston-Berlin, 2000.

[26] R. Rannacher: *Incompressible viscous flow*, Encyclopedia of Computational Mechanics (E. Stein et al., eds), Volume 3 'Fluids', John Wiley, Chichester, 2004.

[27] R. Rannacher: *Adaptive FE eigenvalue approximation with application to hydrodynamic stability*, Proc. Int. Conf. "Mathematical Fluid Mechanics", Estoril, Spain, May 21-25, 2007 (A. Sequeira and R. Rannacher, eds), Springer, Heidelberg, 2009.

[28] R. Rannacher, A. Westenberger and W. Wollner: *Adaptive Finite Element Solution of Eigenvalue Problems: Balancing of Discretization and Iteration Error*, J. Numer. Math 18(4), 303–327 (2010).

[29] Y. Saad: *Iterative Methods for Sparse Linear Systems*, PWS Publishing Company, 1996.

[30] M. Schäfer and S. Turek: *Benchmark computations of laminar flow around a cylinder*, in Flow Simulation with High-Performance Computer II, Notes on Numerical Fluid Mechanics, vol. 52 (Hirschel, E. H., ed.), pp. 547–566, Vieweg, Braunschweig, Wiesbaden, 1996.

[31] L. R. Scott and S. Zhang: *Finite element interpolation of nonsmooth functions satsifying boundary conditions*, Math. Comp. 54, 483–493 (1990).

[32] L. N. Trefethen: *Pseudospectra of linear operators*, In ICIAM 95, Proc. Third Int. Congr. on Industrial and Applied Mathematics (K. Kirchgässner, G. Mahrenholtz, and R. Mennicken, eds.), pp. 401–434, Akademie Verlag, Berlin, 1996.

[33] L. N. Trefethen: *Computation of pseudospectra*, Acta Numerica 8, 247–295, 1999.

[34] L. N. Trefethen and M. Embree: *Spectra and Pseudospectra: The Behavior of Nonnormal Matrices and Operators*, Princeton University Press, Princeton and Oxford, 2005.

[35] L. N. Trefethen, A. E. Trefethen, S. C. Reddy, and T. A. Driscoll: *A new direction in hydrodynamical stability: Beyond eigenvalues*, Tech. Report CTC92TR115 12/92, Cornell Theory Center, Cornell University, 1992.

[36] L. N. Trefethen, S. C. Reddy, and T. A. Driscoll: *Hydrodynamic Stability without eigenvalues*, Science, New Series, Vol. 261, No. 5121, pp. 578–584, 1993.

[37] A. Westenberger: *Numerische Lösung von Eigenwertaufgaben unsymmetrischer partieller Differentialoperatoren*, Diploma thesis, Institute of Applied Mathematics, University of Heidelberg, 2009.